FE-2346-52
Distribution Category UC-91

INFLUENCE OF THE WEAK BEDDING PLANE IN MICHIGAN ANTRIM SHALE ON LABORATORY HYDRAULIC FRACTURE ORIENTATION

Topical Report

Kunsoo Kim and George L. Blaisdell
Department of Geology and Geological Engineering
Michigan Technological University
Houghton, Michigan 49931

Date Published - October, 1979

PREPARED FOR:

THE U. S. DEPARTMENT OF ENERGY

By The Dow Chemical Company
Under DOE Contract No. DE-AC20-76LC10153
(Formerly Contract #EX-76-C-01-2346)

ABSTRACT

Laboratory hydraulic fracturing tests were run on the transversely isotropic Antrim Shale to determine the conditions under which vertical (axial) and horizontal (radial) fractures take place. The testing program was divided into two phases. Tests from the first phase used a nipple packer to fracture shale specimens while the second phase utilized a miniature straddle packer. All of the samples were tested with a vertical stress of 1500 psi. Equal horizontal stresses were varied from zero to 350 psi.

The test results from both phases of the study showed that horizontal fractures were consistently created in samples with a confining (horizontal) stress in excess of 100 psi. Samples subjected to confining stresses less than 25 psi displayed only vertical fractures. Tests in the region between 25 and 100 psi showed either vertical or horizontal failures.

Vertical fractures from both phases of testing showed a preferred fracture direction, suggesting a degree of anisotropy in the plane of bedding.

Existing hydraulic fracturing theory was expanded for transversely isotropic rock to include the effect of two distinct tensile strengths. Experimental breakdown pressure trends were notably similar to those theoretically predicted for both vertical and horizontal failures.

Miniature straddle packer operation was studied in unconfined plexiglass samples to observe the packer's sealing mechanics. Using a soft rubber (60 - 70 durometer) for the inflatable packer elements, it

was found that the packer formed an O-ring type seal with the borehole wall. A low (300 psi) packer set-pressure was all that was necessary to insure that the packer formed a physical plug in the packer-borehole annulus. Borehole pressures of 5000 psi were held by the miniature straddle packer.

Hydraulic fracturing tensile strengths in the plane of bedding were measured for cores from Dow/ERDA well 100 (Sanilac County, Michigan). The tensile strength was found to increase with depth for the upper 165 feet of the formation.

TABLE OF CONTENTS

LIST OF FIGURES AND TABLES

INTRODUCTION

Hydraulic fracturing has been used extensively in the petroleum industry as a stimulation technique to enhance oil and gas well production. The portion of the well to be hydraulically fractured is commonly isolated from the rest of the hole by an inflatable straddle packer. Upon pressurization of the sealed-off section, open fractures are created in the formation. These hydraulically induced fractures act as low resistance migration routes for moving fluids.

The orientation and extent of hydraulic fractures depend on the in-situ stress state and the mechanical properties of the rock. In the case of vertically drilled wells, hydraulic fracture planes commonly assume orientations either parallel or perpendicular to the borehole axis. Fracture planes parallel to the borehole axis are referred to as vertical or axial fractures. Similarly, horizontal or radial fractures are those whose plane is perpendicular to the borehole axis.

Statement of Problem

In initial hydraulic fracturing operations (before 1953) all fractures created were assumed to be oriented horizontally (Clark, 1949). Subsequent work (Hubbert and Willis, 1957), however, proposed that the great majority of hydraulic fractures were, in fact, vertical fractures. Today, little attention is given to the formation of horizontal fractures since it is commonly assumed that most hydraulic fractures are vertical.

The formation of horizontal hydraulic fractures is of particular importance in in-situ retorting, disposal of wastes in geologic formations, and in geothermal energy extraction. Horizontal fractures facilitate interborehole communication and provide not only a pathway for migrating fluids but a greatly increased formation surface area for interaction with the moving fluids.

It is readily apparent that drilling a well to intersect vertical fracture planes could be a difficult task. Should interborehole communication be established for the case of vertical fractures, an additional problem is encountered; vertical fractures cannot always be contained within the pay zone or formation boundaries. This can result in loss of products and possible contamination of ground water.

In the 1950's the Dow Chemical Company became interested in the possibility of extracting hydrocarbons from Michigan's Antrim Shale. An in-situ method of energy recovery was chosen which involved igniting the shale underground to start a burn front. This, in turn, would partially retort the shale and drive off a low BTU gas. The formation was hydraulically fractured in 1977 and 1978 at Dow Chemical's test site in Sanilac County, Michigan. It was hoped that this fracturing would create a secondary permeability capable of transmitting fluids in reasonable quantities. Due to the very weak bedding plane and the essentially flat-lying nature of the Antrim Shale, it was assumed that horizontal hydraulic fractures could be created. The results of field hydraulic fracturing, however, were contrary to those anticipated; only vertical hydraulic fracture planes were confirmed to have been created.

Scope of Investigation

Most previous theoretical and experimental work in hydraulic fracturing has dealt with homogeneous and isotropic rock. For these materials, one tensile strength value and two independent elastic constants are sufficient to characterize the behavior of the rock surrounding the borehole. Since hydraulic fractures are considered tensile failures, the material's tensile strength is incorporated in the theoretical failure criteria.

Most rocks commonly encountered are not homogeneous and isotropic. Layered sedimentary rocks, often the host for hydraulic fracturing, can though, be considered transversely isotropic. Tensile failure in these materials requires the knowledge of two tensile strengths, one in the plane of bedding and the other in a direction perpendicular to bedding, and 5 independent elastic constants. In some types of layered sedimentary rock, in particular shales, the difference between these two tensile strengths is often significant. Failure criteria for transversely isotropic materials with markedly different tensile strength values may indicate that horizontal hydraulic fractures can consistently be created at shallow depths in tectonically relaxed areas as suggested by Sun (1973).

This study is aimed at understanding hydraulic fracture orientation in a transversely isotropic rock. The Antrim Shale was chosen as a representative material because of its pronounced strength anisotropy in tension. Due to the finite diameter of shale speciemens and the rather low outer to inner diameter ratio, the fracture plane orientation could only be studied at its initiation. Previous theoretical hydraulic

fracturing considerations were expanded to include the effect of two distinct tensile strengths. A comparison of laboratory and theoretical failure orientations andp pressures was also attempted.

Two types of packers were used in sealing off the pressurized interval of the borehole. Of interest was the packer's effect on the stress state surrounding the borehole. Using plexiglass samples, the packer's behavior was also studied during borehole pressurization.

LITERATURE SURVEY

The hydraulic fracturing technique was introduced by Clark (1949) for the purpose of oil well production enhancement. Soon after its development, attempts were made to utilize hydraulic fracturing for in-situ stress determination. Hubbert and Willis (1957) present the most thorough of these initial attempts. They propose that the general state of stress underground is not hydrostatic but rather one of unequal principal stresses. Further, it is suggested that since the earth's surface is one along which no shear stresses exist, it is a principal plane. The three principal stress trajectories must then be oriented such that one principal stress is perpendicular to the ground surface and the other two parallel to it. It follows that in regions of gentle topography and large scale simple geologic structures, the principal stresses should be nearly horizontal and vertical. The vertical stress in this case is equal to the weight of the overlying material.

Hubbert and Willis observed that hydraulic fractures are tensile ruptures that orient themselves either vertically or horizontally and propagate in a direction perpendicular to the least compressive principal stress. Analysis of the stress state surrounding a wellbore led to the establishment of failure criteria. Vertical hydraulic fractures could be developed when the borehole fluid reached a pressure equal to or greater than three times the least in-situ horizontal principal compressive stress minus the other in-situ horizontal principal compressive stress. It was noted that pressurization of a cylindrical hole can produce no axial tension unless end effects at well bottoms or packed-off intervals are taken into account. Intuitively, a packed-off hole or an interval containing a well bottom may yield horizontal hydraulic fractures when the wellbore fluid pressure reaches a value equal to or greater than the vertical stress.

Scheidegger (1962) extended the work of Hubbert and Willis to include the rock's tensile strength. He also introduced the idea that the formation may be permeable thus allowing hydraulic fracturing fluids to penetrate the borehole wall before actual breakdown occurs. Scheidegger calculated the failure condition for vertical fracturing for both the penetrating and nonpenetrating situations. For the penetrating condition, however, he assumed the extreme case of formation pore pressure equal to borehole pressure everywhere in the rock.

In a more realistic study of hydraulic fracturing, Kehle (1964) studied the state of stress around a borehole equipped with a straddle

packer. Contrary to past theoretical analyses, this reduced the pressurized interval to a finite length. Kehle adopts a model which assumes the inflatable rubber membranes of the packer can be replaced by two bands of shear stresses acting at the top and bottom of the sealed-off interval (Fig. 1). These shear stresses are the result of frictional forces which are developed by the borehole pressure pushing on the packer element ends. Kehle's packer elements, however, are assumed to be rigid and non-inflatable so that they exert no radial pressure. In between the uniform bands of shear stress the fracturing fluid is represented by a uniform band of radial stress. With this model, he calculates the stress distribution at the borehole wall including the influence of the packers. The ends and the center of the packed-off region are defined as critical regions where fractures will take place. In the central region of the packed-off interval the induced tangential stress is equal to the fracturing fluid pressure and no axial tension is produced. At the packer element - pressurization interval interface the induced tangential stress drops to zero and the induced vertical stress reaches ninety-four percent of the injection pressure. This opened the possibility of defining more realistic failure criteria for horizontal fractures. If created, horizontal fractures would occur near the ends of the interval while vertical fractures would initiate in the central region.

Fairhurst (1964) recognized that hydraulic fracturing was frequently performed on sedimentary rocks. Deposits of this type are commonly

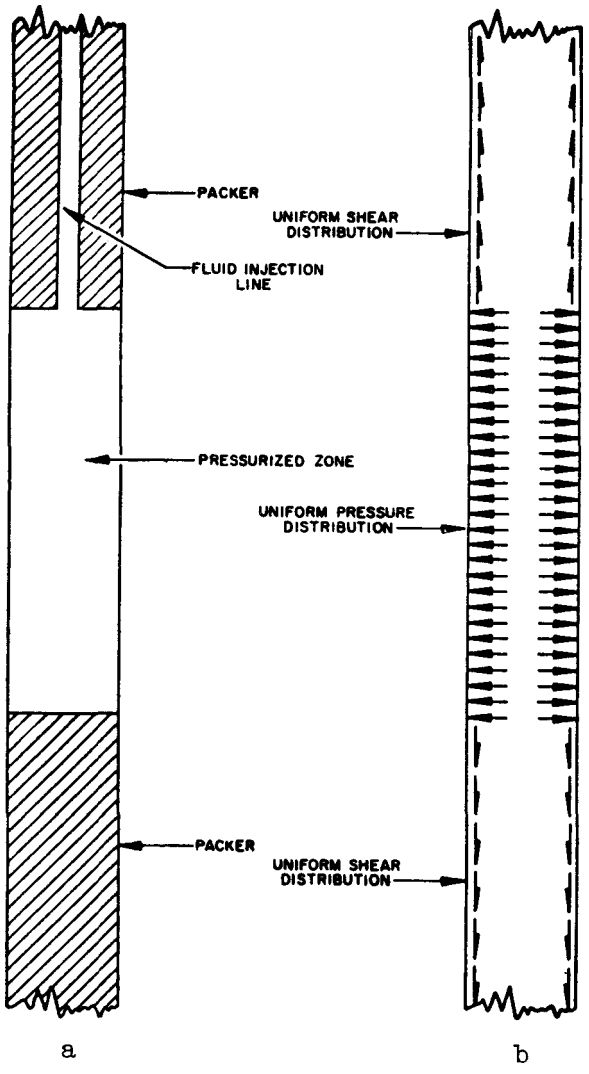

Figure 1. a) Schematic of an inflated straddle packer in a well. b) Kehle's proposed model of the hydraulic fracturing operation. (from Kehle, 1964)

anisotropic with respect to elastic properties and thus violate the assumptions used in previous theoretical developments. Many sedimentary rocks, however, can be regarded as transversely isotropic (uniform properties with respect to rotations about an axis but anisotropic in planes parallel to that axis). For the case of horizontal beds, Fairhurst suggests that a plane strain analysis can be applied around vertically drilled holes. Thus, the stress distribution surrounding a borehole in transversely isotropic rock would be the same as that for an isotropic material.

Haimson (1968) initiated the next significant step in the development of hydraulic fracturing for stress determination purposes. He observed that most rock is permeable and fluid saturated. Pressurization of the borehole results in some leak-off into the formation and thus a lower breakdown pressure is observed. Through thorough experimental and theoretical work Haimson generated accurate failure criteria making it possible to calculate in-situ horizontal stresses in permeable and porous rocks from field hydraulic fracturing data.

Of particular interest to this study was Haimson's use of a miniature straddle packer. It was hoped that horizontal fractures could be initiated with the use of a packer. This would have allowed a check on the validity of Kehle's theoretical model. The great majority of this samples, however, displayed vertical fractures.

Sun (1972) was one of the first to suggest that, especially at shallow depths, the tensile strength of the rock should not be assumed negligable. He also noted that in bedded rocks (especially shales)

there is often a great difference in the tensile strength in directions parallel and perpendicular to bedding (Sun, 1973). The suggestion was made that this difference in strengths may result in the formation of bedding plane hydraulic fractures. Jaeger and Cook (1976, section 8.10) also noted that anisotropy of tensile strengths may have an effect on fracture plane orientations.

Recent literature concerned with hydraulic fracturing has dealt with many facets of the subject. Daneshy (1973a, 1973b) has studied the conditions surrounding generation of inclined failure planes and hydraulic fracturing through cased and perforated wells. His most recent works (1974, 1978) have looked at what happens to the growth of a fracture plane when it encounters a plane of weakness or distinct changes in rock type. Dunn et al. (1978) have conducted an experimental study of the effects of pore pressure in sandstones and shales on hydraulic fracturing tensile strength values. Medlin and Masse (1976) also conducted a laboratory investigation. Their study determined breakdown pressures and fracture plane orientations for several types of limestone. Some of the samples tested contained notched boreholes to aid in the development of horizontal fractures.

The great majority of recent studies have concerned themselves with in-situ stress measuerements by the hydraulic fracturing method (Bredehoeft et al., 1976; Haimson, 1975, 1976, 1978a, 1978b; Zoback and Pollard, 1978). These investigations include both theoretical and experimental (field and laboratory) studies. A new approach to hydraulic fracturing stress

measurements has been suggested by Abou-Sayed et al. (1978). This method of stress determination is based on a fracture mechanics analysis of preexisting cracks in the borehole vicinity.

Although by no means covering all of the material published on hydraulic fracturing, the works cited in this section offer a beginning point for this study. Laboratory experimentation with transversely isotropic materials and a miniature straddle packer may lead to an enhanced understanding of hydraulically induced fractures.

THEORETICAL DEVELOPMENT

General Assumptions and Conventions

In the initial analysis, the material under consideration is assumed to be isotropic, homogeneous, linearly elastic and brittle. The non-hydrostatic in-situ principal stresses are assumed to be oriented such that one stress is vertical and the other two lie in a horizonal plane.

Compressive stresses are considered positive throughout this paper.

Thick-Wall Cylinder Geometry

The borehole and surrounding material is modeled with a thick-wall cylinder geometry (Fig. 2). This model was chosen not only for its relative ease of mathematical manipulation but also for its similarity to the true field situation.

Impermeable Material

Using cylindrical coordinates and assuming $R_2 >> R_1$, $P_1 > P_2$, and no pressurization interval end effects, the radial, tangential and shear

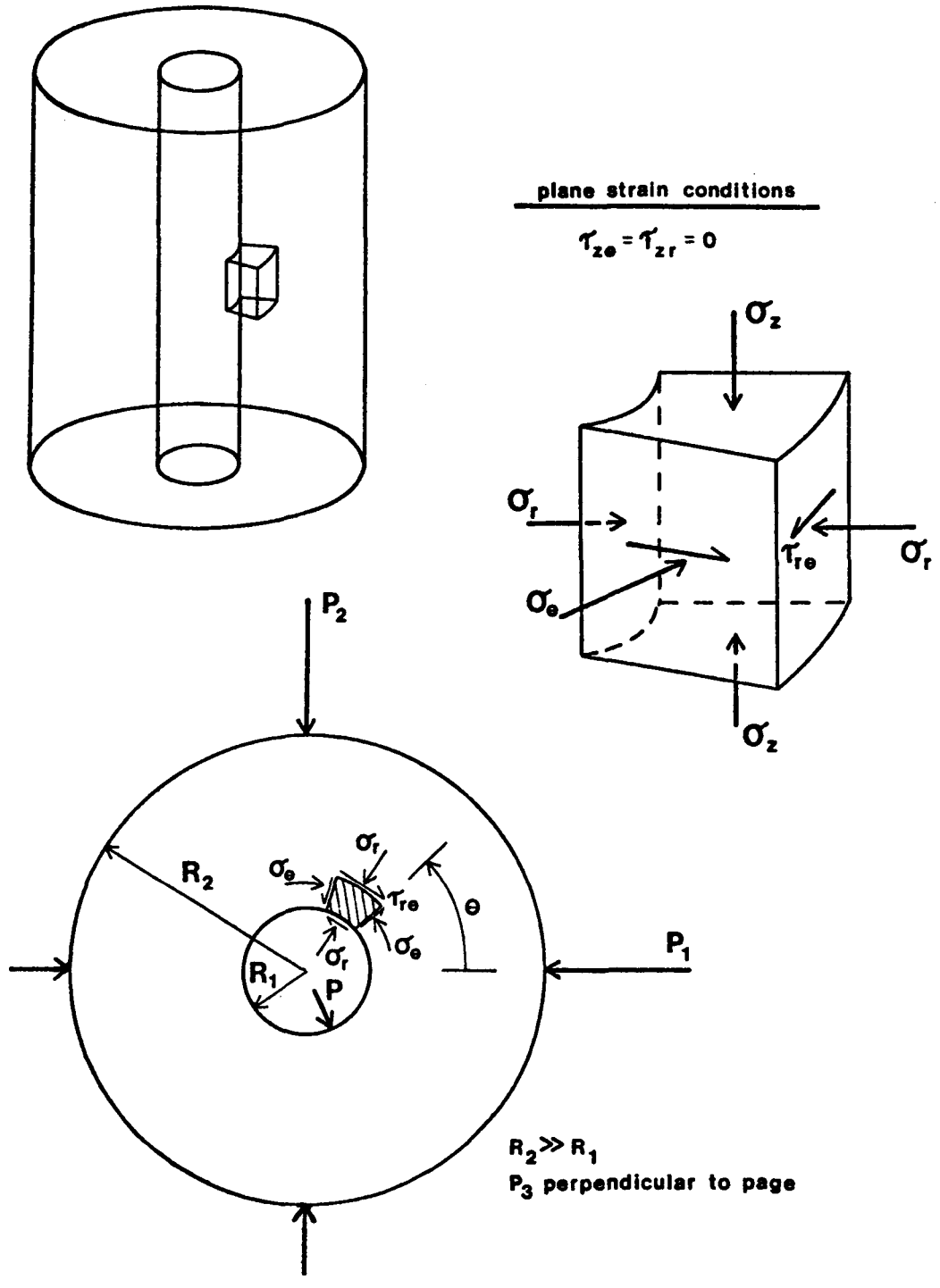

Figure 2. Thick wall cylinder model of borehole and surrounding material showing a small element (near the center of the pressurization interval) and the stresses acting on it.

stresses induced from external and internal pressurization are (from plane strain conditions) (Jaeger and Cook, 1976, section 10.4)

$$\sigma_r = \frac{1}{2}(P_1 + P_2)\left[1 - \frac{R_1^2}{r^2}\right] + \frac{PR_1^2}{r^2} + \frac{1}{2}(P_1 - P_2)\left[1 - \frac{4R_1^2}{r^2} + \frac{3R_1^4}{r^4}\right]\cos 2\theta \quad (3.1)$$

$$\sigma_\theta = \frac{1}{2}(P_1 + P_2)\left[1 + \frac{R_1^2}{r^2}\right] - \frac{PR_1^2}{r^2} - \frac{1}{2}(P_1 - P_2)\left[1 + \frac{3R_1^4}{r^4}\right]\cos 2\theta \quad (3.2)$$

$$\tau_{r\theta} = -\frac{1}{2}(P_1 - P_2)\left[1 + \frac{2R_1^2}{r^2} - \frac{3R_1^4}{r^4}\right]\sin 2\theta \quad (3.3)$$

where R_1 is the borehole radius

R_2 is the external radius

P_1 is the greatest principal in-situ horizontal stress

P_2 is the least principal in-situ horizontal stress

P is the borehole pressure

r is any distance measured from the center of the borehole

θ is the angular distance from P_1.

For a long cylindrical opening with stresses acting at infinity it may be assumed that the radial and tangential displacements are independent of the z direction and that the strain in the z direction is a constant (Jaeger and Cook, 1976, section 10.4). Therefore, the induced axial stress is

$$\sigma_z = E\varepsilon_z + \nu(\sigma_r + \sigma_\theta) \quad (3.4)$$

where ν is Poisson's ratio

E is Young's modulus

ε_z is the axial strain at the borehole wall

Substituting equations (3.1) and (3.2) into (3.4) yields

$$\sigma_z = E\varepsilon_z + \nu\left[(P_1 + P_2) - \frac{1}{2}(P_1 - P_2)\frac{4R_1^2}{r^2}\cos 2\theta\right]. \tag{3.5}$$

Away from the borehole, the stress distribution is not altered by the effect of the well and is therefore independent of r. The axial strain is then

$$\varepsilon_3 = \frac{1}{E}[P_3 - \nu(P_1 + P_2)] \tag{3.6}$$

where P_3 is the in-situ vertical principal stress

ε_3 is the axial strain away from the borehole.

As stated previously, the strain in the z direction is constant, therefore ε_3 equals ε_z at $r = R_1$. Substituting this result into equation (3.6) and solving for P_3 yields

$$P_3 = E\varepsilon_z + \nu(P_1 + P_2) \tag{3.7}$$

It can then be seen that P_3 is equal to the first two terms of the right hand side of equation (3.5). Thus,

$$\sigma_z = P_3 - 2\nu(P_1 - P_2)\frac{R_1^2}{r^2}\cos 2\theta\ . \tag{3.8}$$

At the borehole wall ($r = R_1$) and away from the ends of the pressurized interval, the principal stresses from equations (3.1), (3.2), (3.3) and (3.8) become

$$\sigma_r = P \tag{3.9}$$

$$\sigma_\theta = (P_1 + P_2) - P - 2(P_1 - P_2) \cos 2\theta \tag{3.10}$$

$$\sigma_z = P_3 - 2\nu(P_1 - P_2) \cos 2\theta \ . \tag{3.11}$$

It can be seen that σ_z, the induced axial stress, is independent of the borehole fluid pressure P and thus, in this analysis, horizontal fractures are impossible. For vertical fractures to develop σ_θ must become tensile. Thus $\sigma_{\theta_{min}}$ is found by setting $\theta = 0,\pi$ in equation (3.10), which yields

$$\sigma_{\theta_{min}} = 3P_2 - P_1 - P \ . \tag{3.12}$$

Terzaghi (1943) has shown that in porous materials, failure is governed by "effective stress" levels which can be defined as the total stress minus pore pressure. For impermeable rock, introduction of a borehole and its subsequent pressurization do not change the formation pore pressure levels near the well. Using the prime notation to signifiy effective stresses, they can be expressed as follows:

$$P_1' = P_1 - p_o \qquad P_2' = P_2 - p_o \qquad P_3' = P_3 - p_o \tag{3.13}$$

$$\sigma_r' = \sigma_r - p_o \qquad \sigma_\theta' = \sigma_\theta - p_o \qquad \sigma_z' = \sigma_z - p_o \tag{3.14}$$

where p_o is the undisturbed pore fluid pressure in the formation.

Substituting this result into equations (3.9), (3.11) and (3.12) (and minimizing σ_z) the stress distribution in terms of effective stresses at the borehole wall becomes

$$\sigma'_r = P - p_o \tag{3.15}$$

$$\sigma'_{\theta_{min}} = 3P'_2 - P'_1 - (P - p_o) \tag{3.16}$$

$$\sigma'_{z_{min}} = P'_3 - 2\nu(P'_1 - P'_2) \tag{3.17}$$

Only the induced radial and tangential stresses are functions of the borehole pressure P. As stated previously, hydraulic fractures are tensile ruptures. Thus equation (3.16) must govern failure conditions since equation (3.15) becomes increasingly positive (compressive) with borehole pressurization and equation (3.17) contains no P term. For failure to take place, the induced tangential stress $\sigma'_{\theta_{min}}$ must reach a value equal to the tensile strength T. Substituting this into equation (3.16) results in

$$T = 3P'_2 - P'_1 - (P_f - p_o) \tag{3.18}$$

where T is the material's tensile strength (a negative entity)

P_f is the borehole pressure at failure

Borehole breakdown, resulting in a vertical fracture, will occur when the fluid pressure in the well reaches a critical value P_f defined by

$$P_{f_v} - p_o = 3P'_2 - P'_1 - T \tag{3.19}$$

where P_{f_v} is the borehole breakdown pressure for vertical fractures.

Permeable Material

Haimson (1968) has shown that the complete stress distribution around a borehole drilled into permeable materials can be obtained by superimposing an additional stress field on the impermeable solution. This additional stress field is that caused by borehole fluid flow through the permeable rock. Assuming the same conditions as in the permeable case ($R_2 >> R_1$, $P_1 > P_2$, no end effects) the principal stresses at the borehole wall become

$$\sigma_r = P \tag{3.20}$$

$$\sigma_\theta = P_1 + P_2 - 2(P_1 - P_2) \cos 2\theta - P + \alpha \frac{1 - 2\nu}{1 - \nu} (P - p_o) \tag{3.21}$$

$$\sigma_z = P_3 - 2\nu(P_1 - P_2) \cos 2\theta + \alpha \frac{1 - 2\nu}{1 - \nu} (P - p_o) \tag{3.22}$$

where p_o is the undisturbed pore fluid pressure in the formation

α is the poro-elastic parameter defined by Biot and Willis (1957). It is shown to be equal to $1 - (C_r/C_b)$.

C_r is the material's matrix compressibility

C_b is the material's bulk compressibility.

Pore pressures in permeable rocks are variable. At the borehole wall, the pore pressure is equal to the injection pressure P while at a great distance from the well it is equal to p_o. Effective stresses for permeable and porous rocks can be expressed as follows:

$$P_1' = P_1 - p_o \qquad P_2' = P_2 - p_o \qquad P_3' = P_3 - p_o \tag{3.23}$$

$$\sigma_r' = \sigma_r - P \qquad \sigma_\theta' = \sigma_\theta - P \qquad \sigma_z' = \sigma_z - P \tag{3.24}$$

Substituting this result into equations (3.20), (3.21) and (3.22), the stress distribution in terms of effective stresses at the borehole wall becomes

$$\sigma_r' + P = P \tag{3.25}$$

$$\sigma_\theta' + P = P_1' + P_2' + 2p_o - 2(P_1' - P_2') \cos 2\theta - P + \alpha \frac{1 - 2\nu}{1 - \nu} (P - p_o) \tag{3.26}$$

$$\sigma_z' + P = P_3' + p_o - 2\nu(P_1' - P_2') \cos 2\theta + \alpha \frac{1 - 2\nu}{1 - \nu} (P - p_o) \tag{3.27}$$

Simplifying and evaluating at $\theta = 0,\pi$

$$\sigma_r' = 0 \tag{3.28}$$

$$\sigma_{\theta_{min}}' = 3P_2' - P_1' - \left[2 - \alpha \frac{1 - 2\nu}{1 - \nu}\right] (P - p_o) \tag{3.29}$$

$$\sigma_{z_{min}}' = P_3' - 2\nu(P_1' - P_2') - \left[1 - \alpha \frac{1 - 2\nu}{1 - \nu}\right] (P - p_o) \ . \tag{3.30}$$

A vertical or axial fracture will develop at $\theta = 0,\pi$ when the effective tangential stress $\sigma_{\theta_{min}}'$ becomes great enough to overcome the tensile strength T;

$$P_{f_v} - p_o = \frac{3P_2' - P_1' - T}{2 - \alpha \frac{1 - 2\nu}{1 - \nu}} \tag{3.31}$$

The horizontal failure criterion from equation (3.30), on the other hand, is

$$P_{f_H} - p_o = \frac{P_3' - 2\nu(P_1' - P_2') - T}{1 - \alpha \frac{1 - 2\nu}{1 - \nu}} \tag{3.32}$$

where P_{f_H} is the borehole breakdown pressure for horizontal fractures.

It is assumed that horizontal fractures will be favored when $(P_{f_H} - p_o)$ is less than $(P_{f_v} - p_o)$. Comparing equations (3.31) and (3.32), it is apparent that horizontal fractures would be initiated only if the quantity $3P_2' - P_1'$ is approximately twice P_3' (assuming the quantity $2\nu(P_1' - P_2')$ is negligibly small). Realistically, this situation seldom exists in nature and, once again, vertical fractures are strongly favored.

Packer Effects, Kehle's Model

Kehle (1964), using the model shown in Figure 1, calculated the stress distribution at the borehole wall around a well fitted with a straddle packer. His model was that of an internally and externally pressurized thick-wall cylinder. This calculation was accomplished by superimposing the solution of two separate problems. The effect of the uniform radial pressure (fracturing fluid pressure) and the shear stress bands (rigid packer elements) was determined separately and then combined to give the total effect. The results of Kehle's work are summarized in Figure 3. From this, two distinct regions of the packed-off interval are of interest. The central region, approximately eighty percent, behaves as if no packers were present. Ten percent of the interval on either end of the packed-off region, however, shows an induced axial stress of 0.94 P.

Assuming $R_2 >> R_1$ and $P_1 > P_2$ the following relationships can be established for a packed-off borehole.

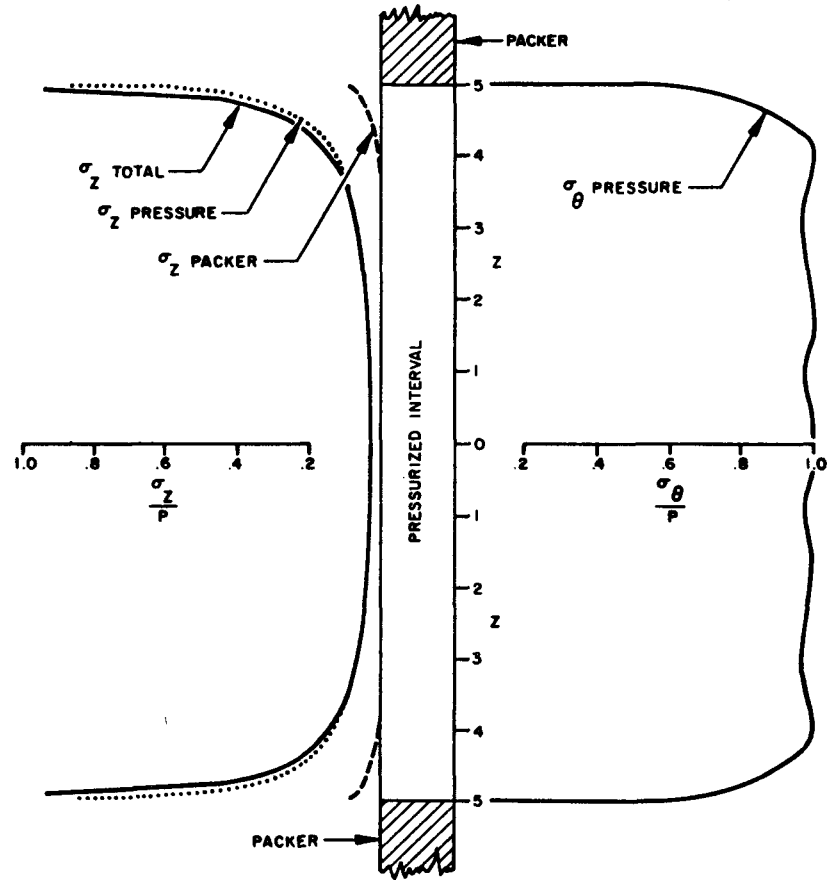

Figure 3. Axial and tangential stresses induced by hydraulic fracturing in a borehole equipped with a straddle packer (from Kehle, 1964).

Impermeable Material

a) Central 80%. The stress distribution in the central 80% of the packed-off interval is identical to the situation that existed when end effects were ignored. Namely, equations (3.15) - (3.17) describe the stress distribution at the borehole wall.

b) Ends of Interval. Due to the influence of the inflatable packer elements, the stress distribution around the borehole near the ends of the pressurized interval for $r = R_1$ becomes (from equations (3.9), (3.10), and (3.11)

$$\sigma_r' = P - p_o \tag{3.33}$$

$$\sigma_\theta' = (P_1' + P_2') - 2(P_1' - P_2') \cos 2\theta \tag{3.34}$$

$$\sigma_z' = P_3' - 2\nu(P_1' - P_2') \cos 2\theta - 0.94(P - p_o) \tag{3.35}$$

Failure criteria can be established by minimizing σ_θ' and σ_z' and setting them equal to the tensile strength of the material. It should be noted that in the central region σ_z' is independent of P and very near the end regions σ_θ' is not a function of P. Thus vertical fractures will initiate in the central region while horizontal fractures will be generated only near the ends of the pressurized interval. This leads to the following fracture conditions for vertical and horizontal failures (in terms of effective stresses):

$$P_{f_v} - p_o = 3P_2' - p_1' - T \tag{3.36}$$

$$P_{f_H} - p_o = \frac{P_3' - 2\nu(P_1' - P_2') - T}{0.94} \tag{3.37}$$

As before, vertical fractures are favored in the majority of in-field situations.

Permeable Material

Haimson (1968) expanded Kehle's theoretical development to include porous and permeable rocks.

a) Central 80%. As was noted above for the impermeable case, the central region behaves as if no packers were present. Equations (3.25) through (3.27) describe the stress distribution at the borehole wall.

b) Ends of Interval. Modification of the stress distribution at the borehole wall due to the packers results in

$$\sigma'_r = 0 \tag{3.38}$$

$$\sigma'_\theta = P'_1 + P'_2 - 2(P'_1 - P'_2)\cos 2\theta - \left[2 - \alpha \frac{1 - 2\nu}{1 - \nu}\right](P - p_o) \tag{3.39}$$

$$\sigma'_z = P'_3 - 2\nu(P'_1 - P'_2)\cos 2\theta - \left[1 - \alpha \frac{1 - 2\nu}{1 - \nu}\right](P - p_o) - 0.94P\ . \tag{3.40}$$

Vertical fractures will develop in the central region and, as before, breakdown will occur when

$$P_{f_v} - p_o = \frac{3P'_2 - P'_1 - T}{2 - \alpha \frac{1 - 2\nu}{1 - \nu}} \tag{3.41}$$

Horizontal fractures, initiating in the end regions, are governed by (from eq. 3.40)

$$P_{f_H} - p_o = \frac{P'_3 - 2\nu(P'_1 - P'_2) - 0.94p_o - T}{1.94 - \alpha \frac{1 - 2\nu}{1 - \nu}} \tag{3.42}$$

Using Kehle's model, no change in vertical fracturing conditions occurs. On the other hand, comparing equations (3.32) and (3.42) it can be seen that for the same material properties and external stress state, a lower horizontal failure pressure is predicted with Kehle's model. This, in effect, increases the possibility of generating horizontal fractures.

The relative relationship between vertical and horizontal failure criteria (from equations (3.36), (3.37), (3.41) and (3.42) for impermeable and permeable isotropic materials is shown in Figure 4. An in-field situation is assumed here (P_1, P_2, P_3, p_o) along with the required material properties (ν, T, α). These assumed quantities are believed to represent realistic values for a sedimentary rock in a tectonically relaxed area. To simplify the plot, the horizontal principal stresses (P_1 and P_2) are set equal to each other. This is commonly the case in laboratory studies where cylindrical samples are subjected to an axial load and a confining pressure. It can be seen that breakdown pressures are significantly reduced in a permeable material. It is also shown that the transition from vertical to horizontal fractures in a sample with 1000 psi axial stress does not take place until a confining pressure of between 500 and 700 psi is reached.

Transversely Isotropic Material

The theoretical development of failure criteria for transversely isotropic materials will limit itself to the consideration of two distinct tensile strengths. It will be assumed here that the stress-strain

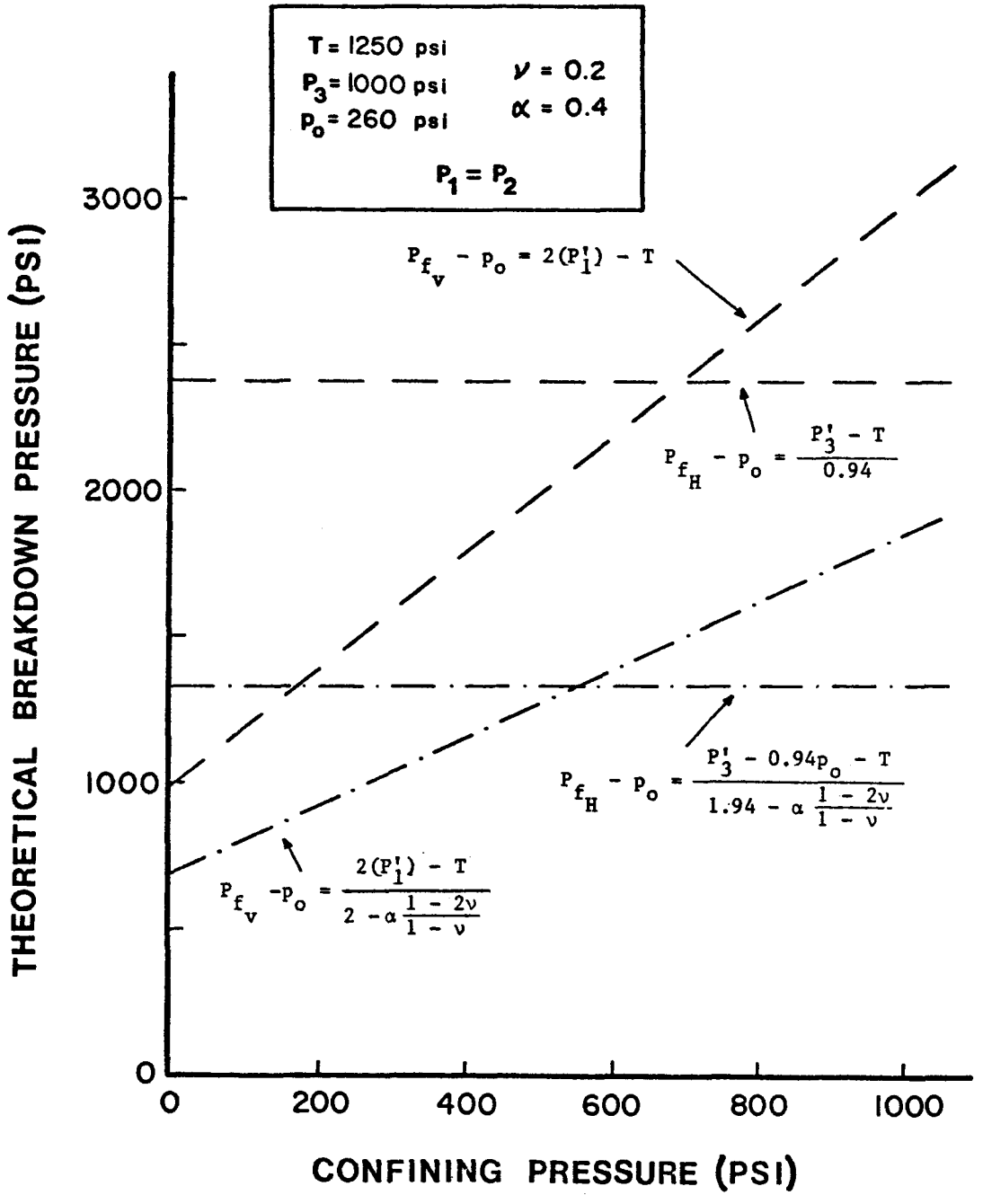

Figure 4. Theoretical vertical and horizontal breakdown pressures for permeable and impermeable isotropic materials.

equations for homogeneous and isotropic materials are generally valid for transversely isotropic materials (Sun, 1969). Since the initial development was based on vertical and horizontal principal stress trajectories, and it was stated that this was the case in tectonically relaxed areas, the bedding plane will be considered horizontal. A vertically drilled well will then intersect the bedding plane at a 90° angle. The tensile strength of the formation acting to part the bedding plane T_1 (perpendicular to bedding) will be directed parallel to the borehole axis. In the plane of bedding, the tensile strength T_2 acts perpendicular to the borehole axis. It is apparent that T_1 is the important tensile strength in horizontal fracturing. On the other hand, calculations leading to vertical failure criteria are governed by T_2.

Inclusion of two tensile strengths in the failure conditions for impermeable materials fractured with a packer yields the following:

$$P_{f_v} - p_o = 3P_2' - P_1' - T_2 \tag{3.43}$$

$$P_{f_H} - p_o = \frac{P_3' - 2\,(P_1' - P_2') - T_1}{0.94} \tag{3.44}$$

Likewise, for permeable materials

$$P_{f_v} - p_o = \frac{3P_2' - P_1' - T_2}{2 - \alpha \frac{1 - 2\,\nu}{1 - \nu}} \tag{3.45}$$

$$P_{f_H} - p_o = \frac{P_3' - 2\nu(P_1' - P_2') - 0.94p_o - T_1}{1.94 - \alpha \frac{1 - 2\nu}{1 - \nu}} \tag{3.46}$$

Creating an in-field set of conditions for a transversely isotropic material gives the horizontal and vertical failure conditions shown in Figure 5. The material properties chosen here are believed to be representative of a shale such as the Antrim. The transition point from vertical to horizontal fractures is now displaced to a confining pressure between 100 and 200 psi. This suggests that it may be possible to consistently create horizontal fractures at shallow depths in distinctly anisotropic rock.

EXPERIMENTAL APPARATUS AND PROCEDURES

Sample Collection and Preparation

The samples used in this study were obtained from two large quarry blocks collected from the Paxton clay quarry near Alpena, Michigan. The Antrim Shale at Paxton quarry is easily identified as mineralogically belonging to Bennett's (1978) lithofacies III; many bioturbated horizons were recognizable. Each block was approximately 4 1/2 feet square and 3 feet high. The blocks were taken from the west wall of the quarry and were specifically chosen for their relative lack of bedding plane fractures. Previous collection of smaller blocks proved unsatisfactory as a large number of cores of adequate length could not be recovered from them. This was primarily due to the presence of numerous natural bedding plane partings which appeared to increase in frequency as quarry block thickness (measured perpendicular to bedding) decreased. The quarry slabs were taken from talus piles which completely obscured all but the upper

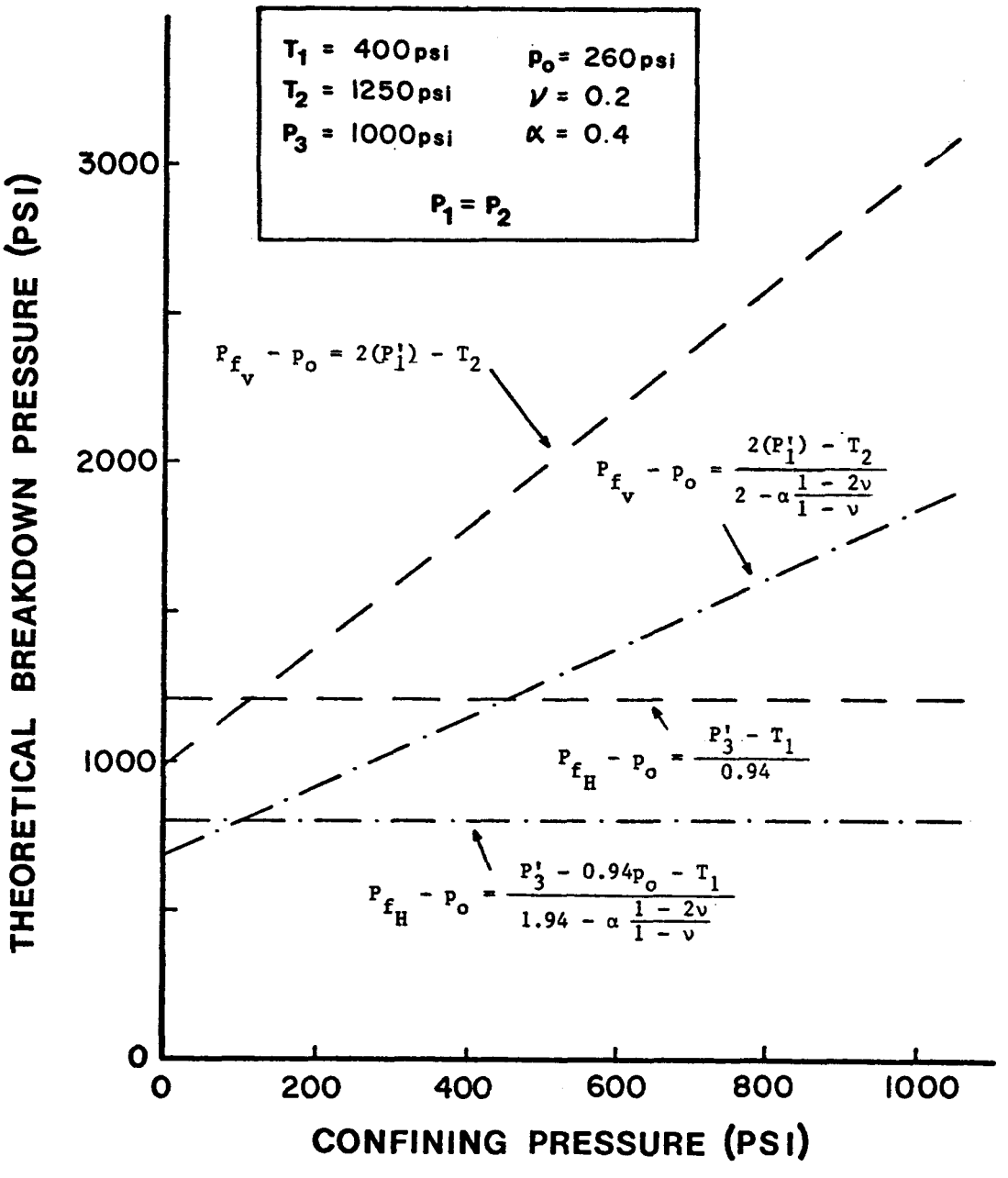

Figure 5. Theoretical vertical and horizontal breakdown pressures for permeable and impermeable transversely isotropic materials.

few feet of the working face. Thus, it was not possible to orient the blocks.

Sample preparation began with the construction of a temporary mud pit which surrounded the block during drilling. Each block was cored with a portable drill mounted on a movable wooden stand (Fig. 6) to yield samples of the desired geometry. Water was used as the drilling fluid. Although the stand was slightly unstable, smooth-sided straight cores were recovered by using slow drilling rates. Extreme care had to be used in removing freshly drilled samples from their "sockets"; lifting them from their top invariably caused the sample to break along a bedding plane. The first block was drilled to yield 2.150 inch cores (from now on called 2-1/8 inch cores). Using a 3-1/2 inch core bit, the second block was drilled to yield samples approximately 3.226 inches in diameter. A directional convention was assumed for each block so that all the samples from a particular block could be oriented relative to each other. No relative orientation was possible between the two blocks.

Following coring, each sample was allowed to air dry before it was wrapped its full length with masking tape. This helped to prevent cracking of the cores during handling and subsequent preparation. Each sample was rough cut to a prescribed length (4 inches for 2-1/8 inch cores and 3-3/4 inches for 3-1/2 inch samples). The simulated borehole was then drilled in the center of each sample with a drill press. A guide bushing was used to insure accurate centering of the borehole in

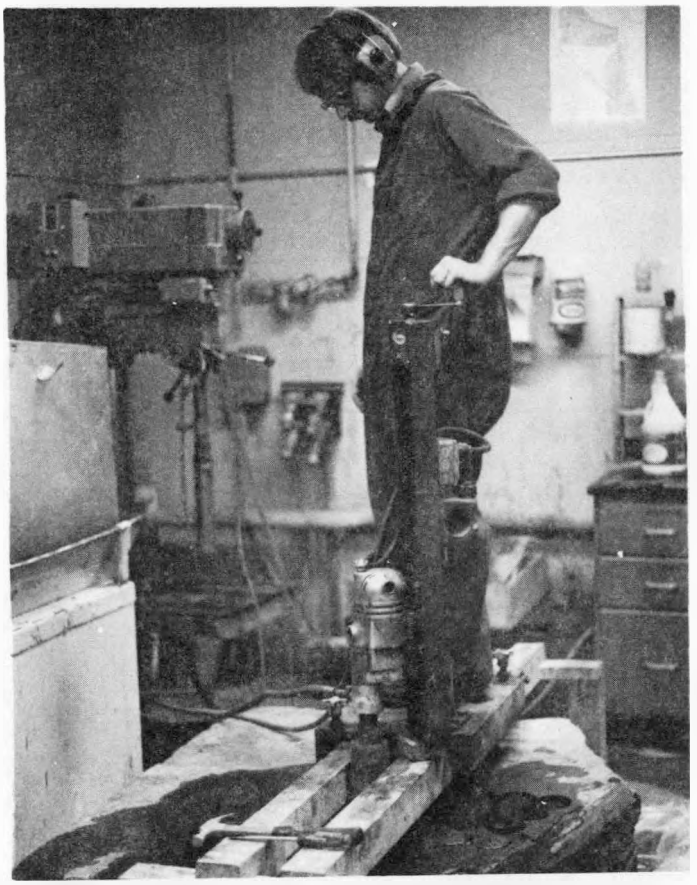

Figure 6. Quarry block coring with portable drill on wooden stand.

the sample and borehole straightness was achieved using a special jig, clamped to the drill press table, which held each sample perfectly upright. Cores 2-1/8 inches in diameter were drilled with a masonary bit through 2/3 of their length, leaving a 1/4 inche hole at their centers. Drilling fluid circulation was not able to be maintained adequately with the masonary bit. This resulted in the development of bedding plane fractures near the base of the borehole where circulation was the poorest. These "prefractures" were present in most 2-1/8 inch cores. Samples with a 3-1/2 inch diameter were undercored their full length using a diamond drill bit. The borehole left in this case was 0.800 inches in diameter.

All samples were then surface ground to insure parallelism of their ends. The same jig used for drilling the borehole was used for surface grinding thus insuring that the sample ends became perpendicular to the cored walls. Parallelism was achieved within 0.003 inches in all cases.

Testing Equipment for External Loading and Data Acquisition

An MTS closed-loop servo-controlled test system interfaced with a Digital pdp 11/04 computer was used to run all tests (Fig. 7). A two-channel controller unit* provided linking between the computer and hydraulics. One channel was used to operate the million-pound load frame and the second channel controlled a 40,000 psi pressure intensifier† (Fig. 8). The servo-controlled pressure intensifier has a 22 cubic inch capacity and can be operated under pressure control or volume control.

*MTS models 406.11 (with DC conditioner) and 442.11

†MTS model 286.02 (with high pressure booster)

Figure 7. MTS test system. From left, hardcopy unit, cathode-ray-tube terminal, load frame, controller unit and computer.

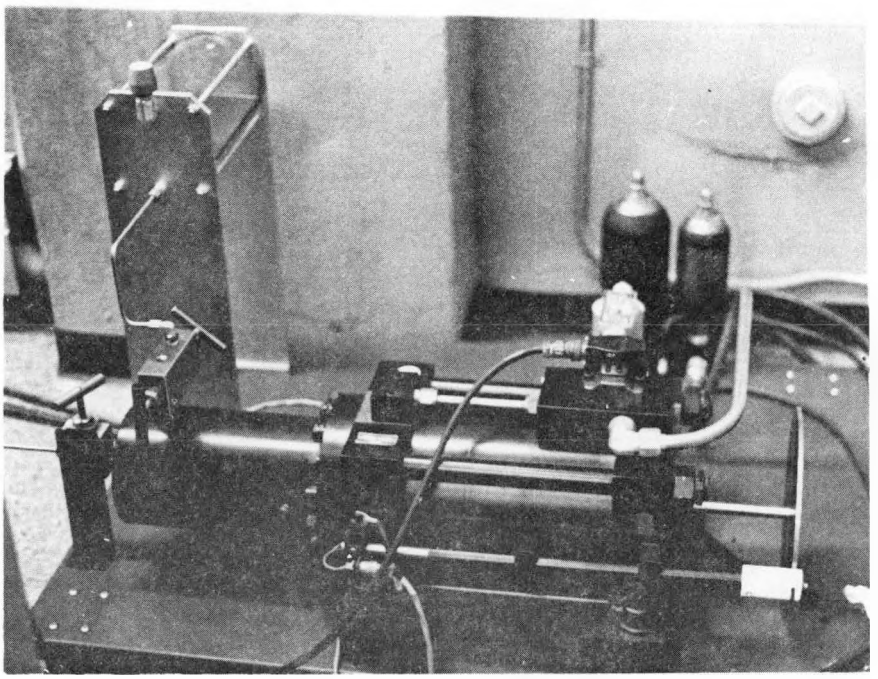

Figure 8. MTS 40,000 psi pressure intensifier.

Axial, circumferential (confining) and borehole pressures were continuously monitored by the system. During unconfined tests the packer pressure was also monitored by the system. For all confined tests, however, the packer pressure was measured with a gage. As a back-up to the main system, a two-channel time-base oscillographic recorder* was used to record confining and borehole pressures. This allowed the detection of sample failure during confined tests since visual observation was not possible due to the triaxial (confining) cell. The oscillographic recorder also provided the borehole breakdown pressure in the event the main system malfunctioned and a data set was lost.

Feedback for the pressure intensifier was provided by a pressure transducer† located on the hydraulic line leading to the borehole (Fig. 9). The borehole transducer was in control on channel one at all times during the test. The confining transducer* only monitored pressure in the triaxial cell. Since only one pressure source (the pressure intensifier) was available to generate confining and borehole pressures, valve manipulation was necessary during each test.

A load cell†† provided feedback for the second channel which controlled the load frame (axial stress).

Testing was accomplished through a computer program (Appendix I). Initial input to the program included sample parameters (specimen number,

---

* Hewlett Packard 7402A recorder
† BLH model 413750 (0 - 30,000 psi)
** BLH model 413748 (0 - 10,000 psi)
†† Strainsert model FL150C-25GK (0 - 150,000 lb_f compression)

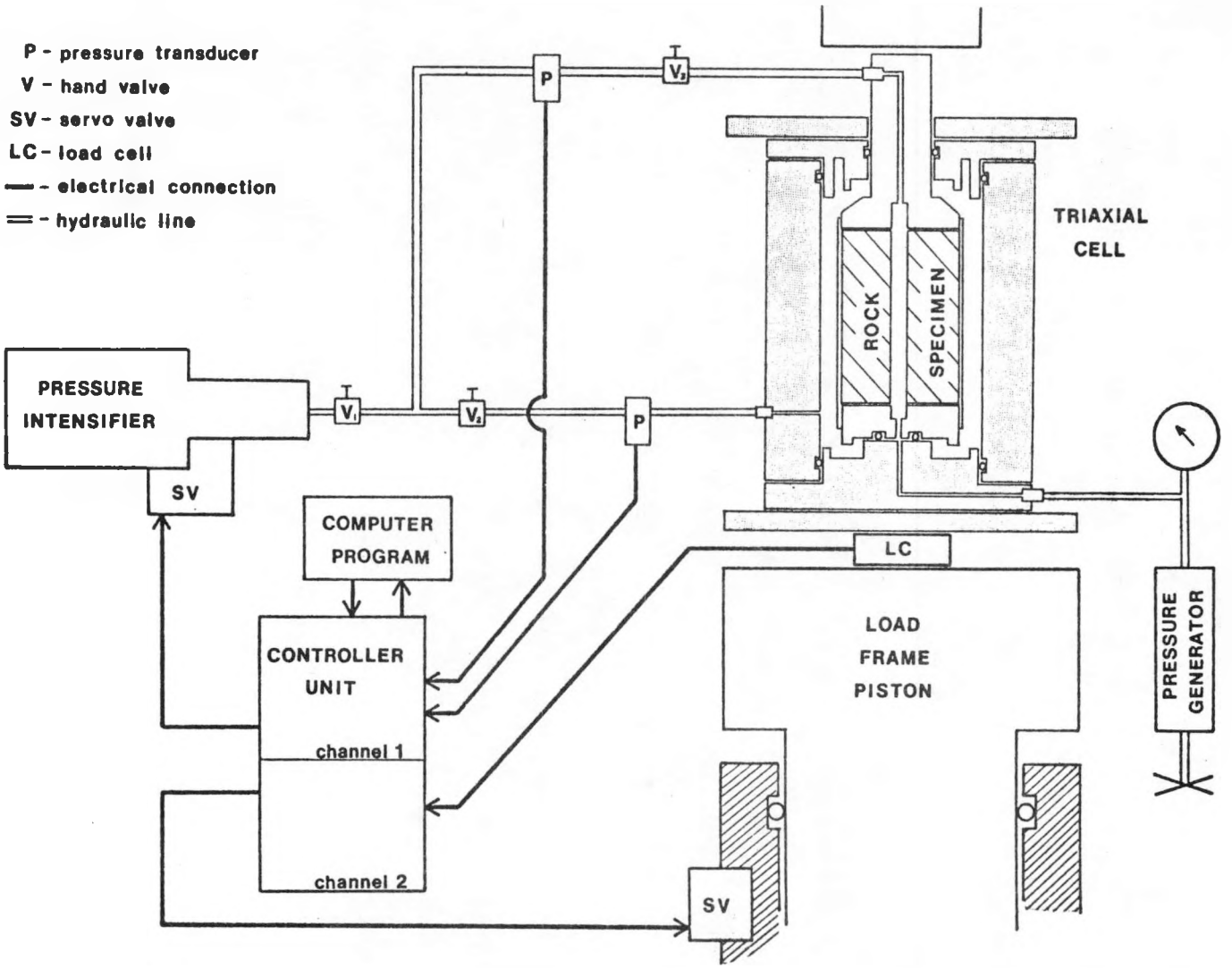

Figure 9. Schematic of testing circuit used for laboratory hydraulic fracturing. Shown here with 30,000 psi triaxial cell for miniature straddle packer tests.

inner and outer diameters) and loading parameters (desired axial and confining stresses). The loading portion of the program was divided into two halves. The first half simultaneously increased the confining and axial stresses linearly. During this half of the test, valves one and two (V_1 and V_2 in Figure 9) were open and valve three (V_3) was closed. Each load increased to its previously defined level where it then remained constant. Valve two was then closed and remained closed for the remainder of the test.

Confining pressures were applied through two types of triaxial cells. A simple triaxial cell*, shown in Figure 10, was used for 2-1/8 inch samples (nipple packer tests). For 3-1/2 inch samples (straddle packer tests), a 30,000 psi Structural Behavior Engineering Laboratories triaxial cell† was used (Fig. 11, schematic in Fig. 9). This cell not only allowed the use of 3-1/2 inch diameter specimens, but contained a passageway in its base for the transfer of packer inflation fluid.

To begin the second half of the test, the intensifier was returned to zero pressure and valve three was opened. (The axial load and confining pressure still remained at their previous levels.) The miniature straddle packer was then "set" (packer elements inflated to desired pressure) in tests with 3-1/2 inch samples. The pressure for the packer was provided by a 10,000 psi hand pressure generator** (Fig. 12). The borehole pressure was then linearly increased at a rate of 65 psi per second until failure occurred.

---

* Terrametrics triaxial confinement chamber (0 - 10,000 psi)
† Rockcell model 30 (0 - 30,000 psi)
**HIP Model 62-6-10 (0 - 10,000 psi, 30 cc volume)

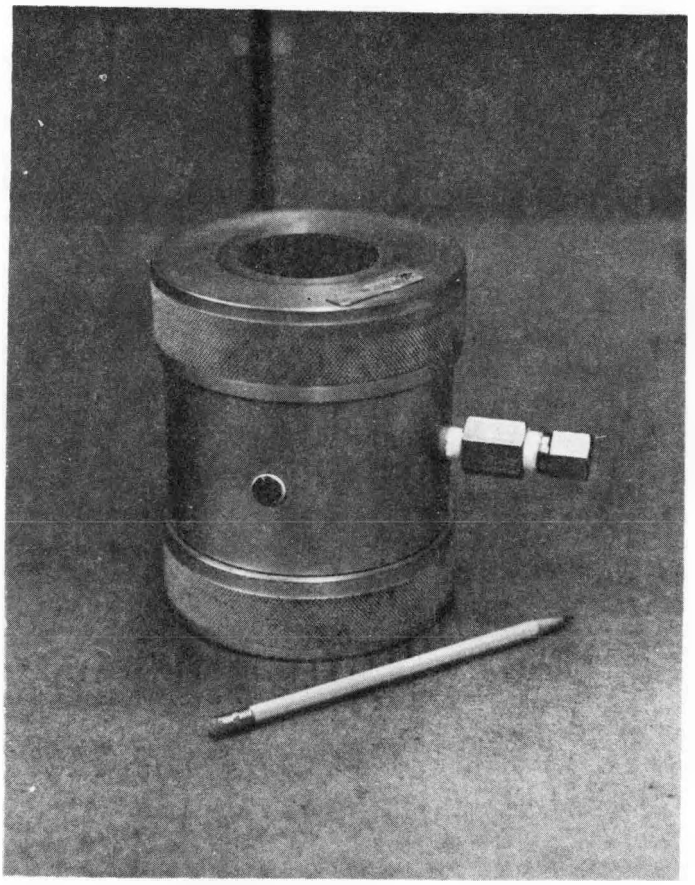

Figure 10. Small triaxial cell (10,000 psi) for nipple packer tests.

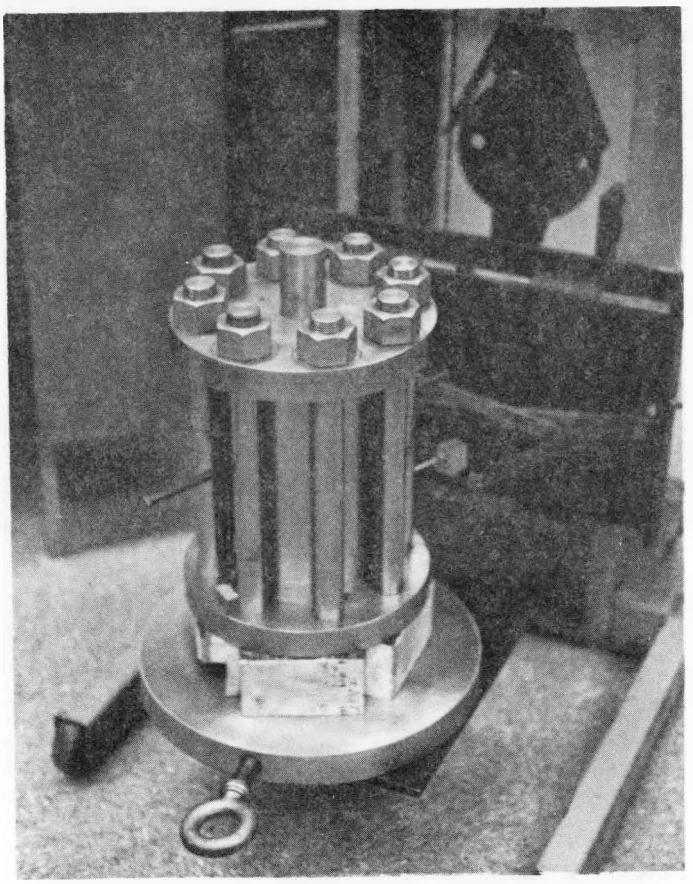

Figure 11. Large triaxial cell (30,000 psi) for straddle packer tests.

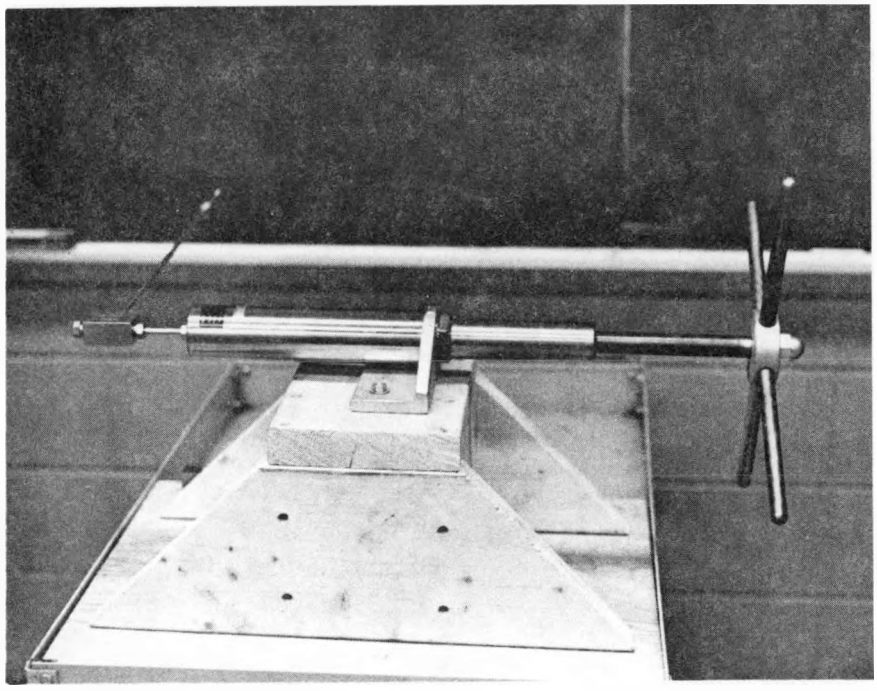

Figure 12. Hand pressure generator for straddle packer inflation.

Data acquired by the program during the test was plotted on a cathode-ray-tube display*. The graphing was performed by plotting subroutines in the program. These subroutines were capable of displaying plots of axial, confining or borehole pressures versus time. A fourth subroutine made it possible to accurately determine the failure pressure from the borehole pressure-time plot. A hardcopy unit† was used to obtain permanent copies of these plots.

The data for each test was stored on a floppy disk where it could be retrieved and plotted by a separate program.

Investigation with Nipple Packer

2-1/8 inch diameter samples with a 1/4 inch borehole were hydraulically fractured with a nipple packer (Fig. 13). The packer screwed into a modified end piece which allowed the transfer of fracturing fluid. The pressurization section of the borehole was sealed-off at the top by the lower O-rings on the nipple packer. The rock itself (end of the borehole) served as the lower extent of the pressurization interval.

Tests conducted on plexiglass samples (geometrically identical to the Antrim specimens) confirmed that the O-rings did seal against the borehole wall. Also, several rock specimens which broke vertically did not expose any of the fracture trace on their top surface; the only fracture traces were formed along cylinder walls. The pressurized interval was thus assumed to be isolated in the central region of each specimen.

* Tektronix model 4010-1
† Tektronix model 4631

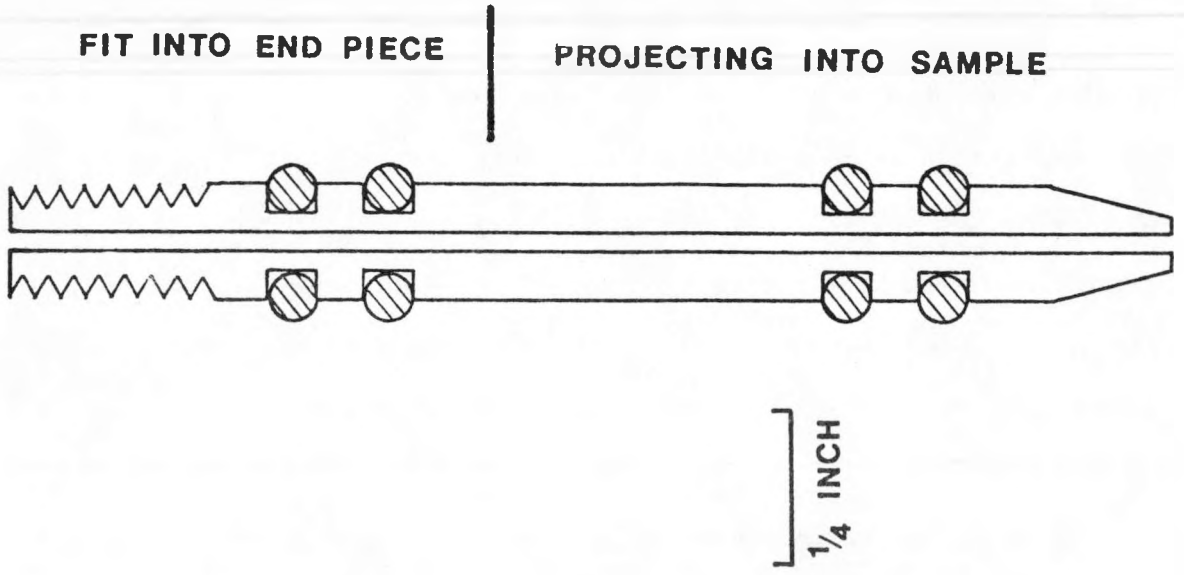

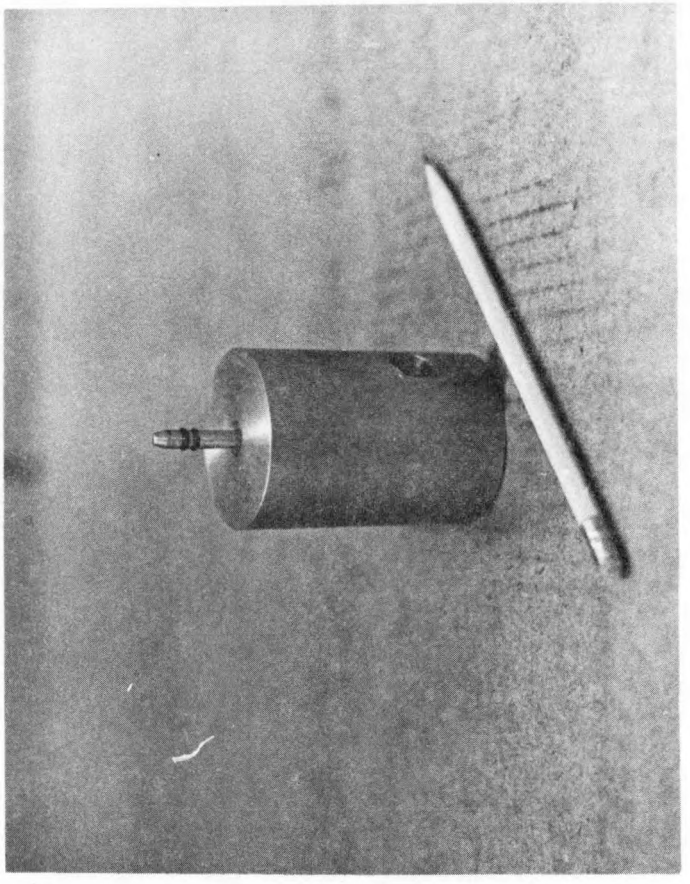

Figure 13. Nipple packer, screwed into end piece and schematic.

Samples taken from one quarry block were used in this series of tests. All specimens were thus mineralogically as identical as possible. The testing program used an axial stress of 1500 psi for all samples. Confining pressures were varied from zero to 350 psi. As numbers permitted, several samples were tested at each load level. The greatest concentration of samples was tested in the unconfined state to establish a representative value for the hydraulic fracturing tensile strength in the plane of bedding. Borehole breakdown pressures and fracture orientations were recorded for each sample and later analyzed.

Investigation with Miniature Straddle Packer

A miniature straddle packer (Fig. 14) was designed to imitate, as closely as possible, a straddle packer used in field hydraulic fracturing operations. Modified end pieces (Fig. 15) which attached to the top and bottom of the miniature straddle packer transmitted fluids for fracturing and pressurization of the packer elements. The end pieces also applied the 1500 psi axial stress to each specimen. The inflatable rubber membranes were expanded with water soluble oil to seal-off a central interval in the sample. Hydraulic oil was then pumped into the area between the rubber membranes until failure took place.

Initial operation of the miniature straddle packer utilized unconfined plexiglass samples to allow direct visual observation. The epoxied contact between the rubber membranes and the steel packer failed numerous times causing the rubber packers to deflate. After many trials

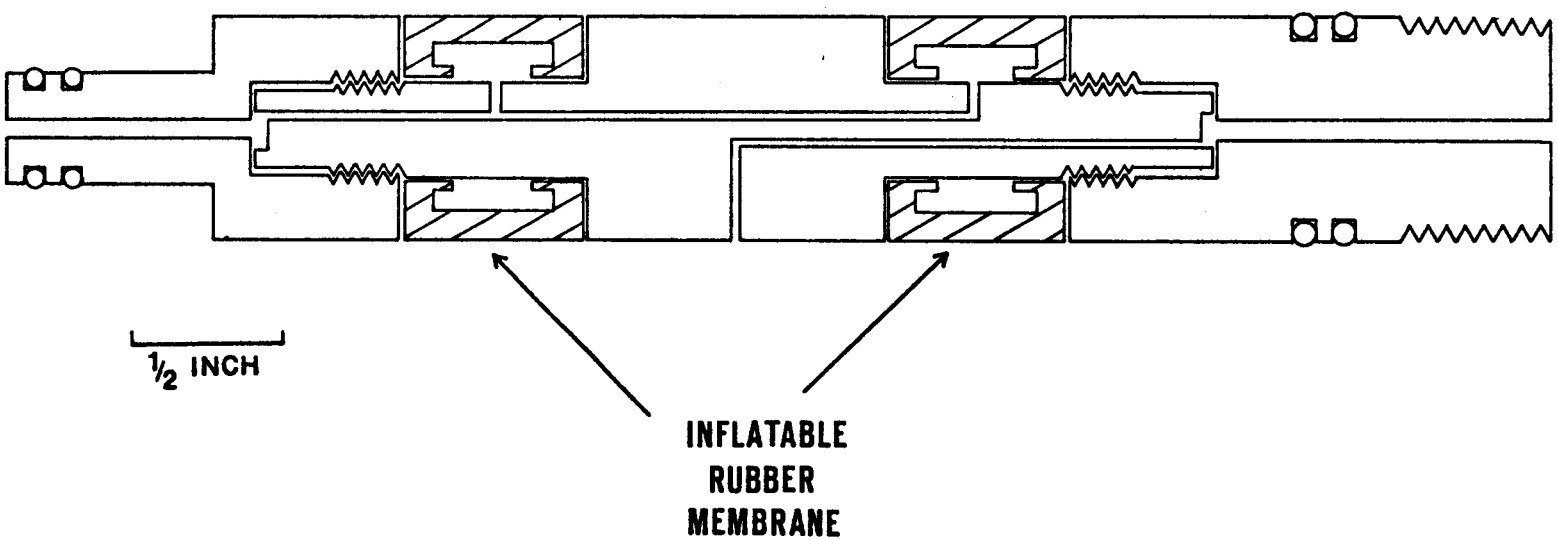

Figure 14. Schematic of miniature straddle packer.

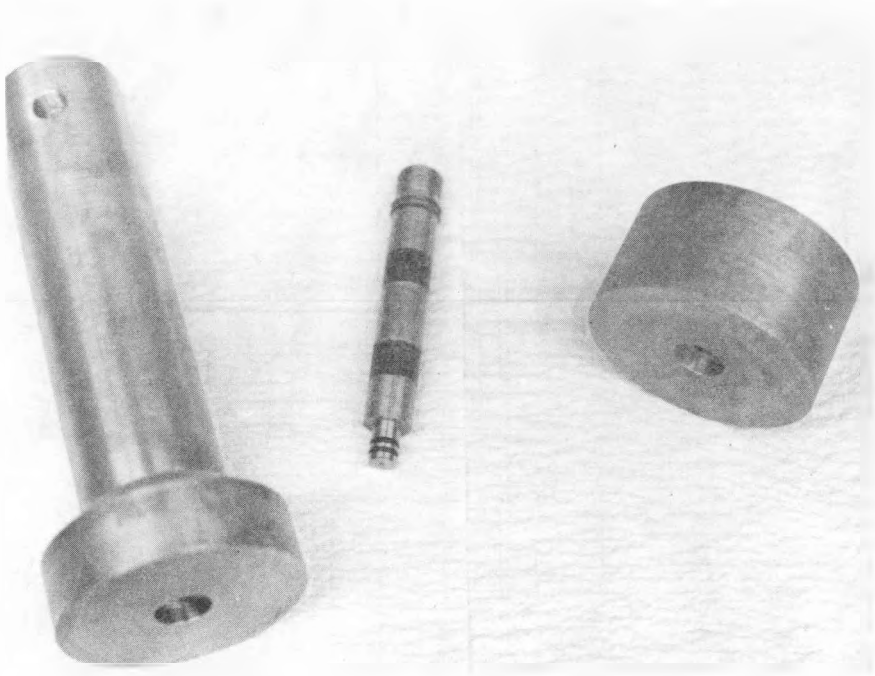

Figure 15. Miniature straddle packer and modified end pieces for laboratory hydraulic fracturing.

with various epoxy and adhesive types, Scoth-Weld Structural Adhesive 1838 was found to hold best, long enough to run from 20 to 40 tests without failing. Careful preparation of the rubber and steel contact points was necessary, however, to insure this bonding quality. Typical strain gage mounting procedures were used to prepare these surfaces.

When operational, the miniature packer was again used in unconfined plexiglass samples to study its sealing mechanics. Sealing failure was called extrusion and was defined to have taken place when the borehole pressurizing fluid leaked past either the top or bottom inflatable membrane. It was assumed that this indicated the rubber packer elements were not initially set at a high enough pressure to contain the fracturing fluid to the pressurization interval. It was felt that a plot of packer set-pressure versus its corresponding extrusion pressure could be generated. This packer failure curve would allow one to choose a minimum packer set-pressure for a given anticipated breakdown pressure. Using this curve would insure that the packer was not set at an unnecessarily high pressure. An excessive set-pressure would perhaps result in premature borehole breakdown. (A failure of this type will always yield a vertical fracture.)

The testing procedure with the miniature straddle packer was identical to that for the nipple packer. Samples used for this test were all taken from the second large quarry block. Each sample was jacketed with heat-shrinkable tubing (Fig. 16) before being placed in the large triaxial cell. Due to the excessive amount of time required for set-up and take-

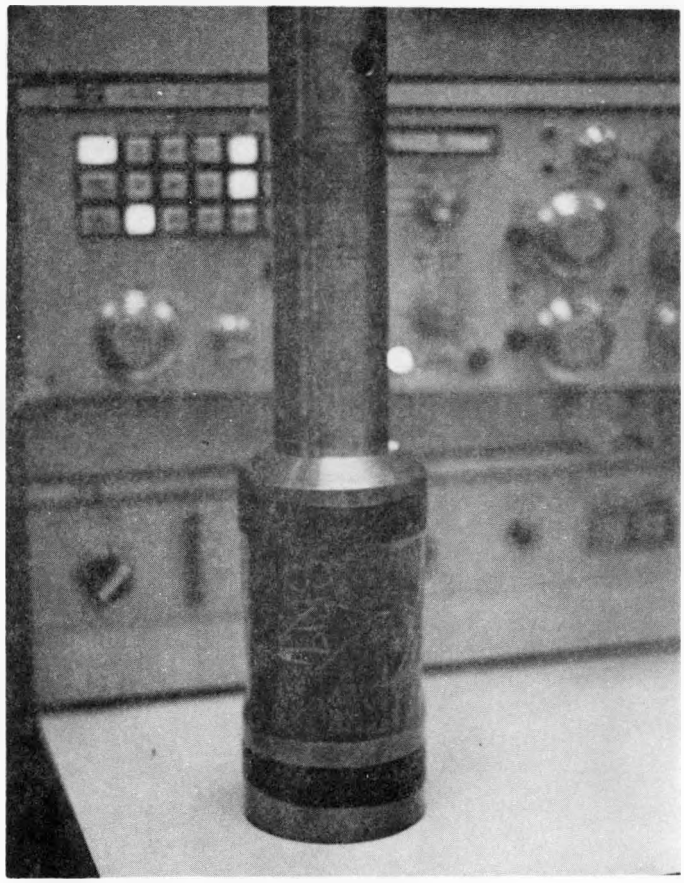

Figure 16. Sample jacketed with heat-shrinkable tubing ready for straddle packer test.

down of the triaxial cell for each sample, a minimum number of samples was tested. Packer set-pressure, borehole breakdown pressure and fracture orientation were recorded and later analyzed.

The miniature straddle packer was also used to determine the tensile strength (T_2) of some cores taken from Dow/ERDA well 100 (Appendix II).

RESULTS OF INVESTIGATION

Results of Nipple Packer Investigation

Packer Operation

The nipple packer was first tested using plexiglass samples of the same dimensions as the rock specimens to be tested later. In the unconfined state, this testing allowed visual observation of the sealing quality of the packer's O-rings. With hard O-rings (90 durometer) the packer was capable of holding a borehole pressure of about 500 psi. After leakage past the O-rings, oil filled the region between the top end piece and the O-rings and the entire length of the borehole was then pressurized.

O-rings of 65 - 70 durometer allowed the nipple packer to hold a substantially higher pressure. Borehole pressures as high as 5000 psi were easily reached. During borehole pressurization a typical O-ring seal developed; the O-rings formed a physical plug in the annulus between the nipple packer and the borehole wall. Sealing failure of the nipple packer occurred only when the O-rings extruded. Extrusion took place when the majority of the O-rings cross-section was forced into the annulus.

Following extrusion, fluid was capable of leaking past the O-rings. A sudden drop in pressure was noted at extrusion as oil filled the annulus above the O-rings. The servo-controlled system recovered very quickly, however, and only a small spike was plotted on the oscillographic recorder. O-rings experiencing extrusion were permanently stretched a slight amount and failed at a lower pressure during their next use. Thus, a new set of O-rings was mounted on the nipple packer after any test that resulted in extrusion.

During nipple packer tests on rock samples, the oscillographic recorder was visually monitored to detect O-ring extrusion. If a small spike appeared in the record, borehole pressurization was discontinued. The O-rings were then replaced and the sample was retested to failure. This monitoring was assumed to insure that the pressurization interval remained isolated from the ends of the sample.

Hydraulic Fracturing Results

Seven quarry block samples were tested unconfined to determine the hydraulic fracturing tensile strength T_2 (in the plane of bedding). All seven samples broke vertically despite the fact that four of them contained distinct horizontal prefractures. During borehole pressurization, leak-off occurred through these horizontal planes (Fig. 17). The amount of leak-off was variable depending on the extent and number of prefractures. The borehole pressurization rate was kept constant despite leak-off, by the servo-controlled system. The three intact samples provided the highest

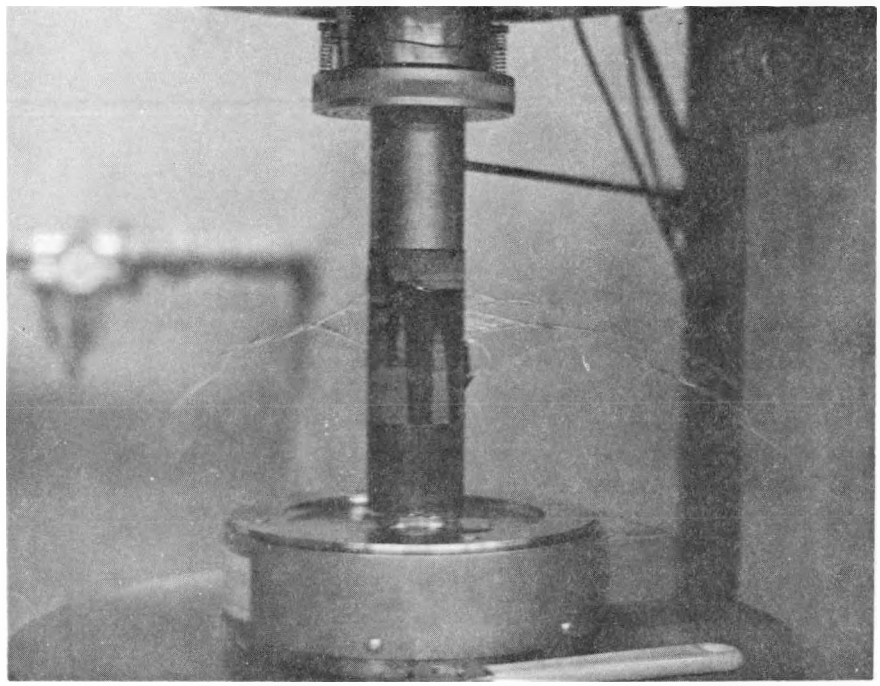

Figure 17. Vertical fracture occurring in unconfined prefractured sample. Note leak-off from horizontal prefractures.

borehole breakdown pressures for unconfined testing (Table 1). These samples also showed little variation in their failure pressures. The average breakdown pressure for intact specimens indicates a tensile strength value of 3660 psi (from equation (3.19) or (3.43)). This is probably a more representative figure for the in-situ vertical hydraulic fracture tensile strength than 3040 psi which is found by averaging all seven breakdown pressures. The amount of leak-off experienced in these tests would probably not be present in field fracturing of the Antrim Shale.

Three samples were tested at confining pressures of 25, 50, 75, and 100 psi. The remaining samples were tested at confining pressure levels from 150 to 350 psi. Breakdown pressure and fracture orientation are recorded for each sample in Table 2.

Confined tests on samples which yielded vertical fractures showed a sudden drop in borehole pressure at the instant of borehole breakdown. Creation of the fracture plane established communication between the borehole fluid and the flexible triaxial cell membrane which transmitted confining pressure. Since the confining fluid had a fixed volume (due to closing of the hand valve leading to the triaxial cell; Figure 9) and the borehole fluid was at a much higher pressure, an immediate increase in the confining pressure was noted at breakdown (Fig. 18a). Borehole breakdown pressure for vertically fractured specimens was defined as the maximum borehole pressure reached before its sudden drop and the corresponding rapid increase in confining pressure.

TABLE 1

Hydraulic Fracturing Tensile Strength in the Plane of Bedding for 2-1/8 inch Antrim Shale Cores from Paxton Quarry Block 7

Sample	Axial Stress (psi)	Confining Pressure (psi)	Breakdown Pressure (psi)	Fracture Orientation
S71*	1500	0	3120	vertical
S72*	1500	0	2190	vertical
S73*	1500	0	1750	vertical
S74	1500	0	3640	vertical
S75	1500	0	3580	vertical
S76*	1500	0	3190	vertical
S77	1500	0	3760	vertical

*Indicates samples with preexisting horizontal fractures

TABLE 2

Hydraulic Fracturing Results for 2-1/8 inch Antrim Shale Cores from Paxton Quarry Block 7

Sample	Axial Stress (psi)	Confining Pressure (psi)	Breakdown Pressure (psi)	Fracture Orientation
S724*	1500	25	3820	vertical
S725*	1500	25	3110	vertical
S732*	1500	25	3280	vertical
S714	1500	50	4640	vertical
S717*	1500	50	3300	vertical
S720	1500	50	3910	vertical
S711*†	1500	75	2510	horizontal
S718*†	1500	75	1400	horizontal
S733	1500	75	2600	horizontal
S723*	1500	100	2190	horizontal
S727*	1500	100	4290	vertical
S736*†	1500	100	1570	horizontal
S716*†	1500	150	1500	horizontal
S726*†	1500	200	1400	horizontal
S742	1500	200	2730	horizontal
S743*	1500	250	2030	horizontal
S712*†	1500	300	1400	horizontal
S731*†	1500	350	1400	horizontal

*Indicates samples with preexisting horizontal fractures

†Indicates breakdown pressure was defined by 25% increase in confining pressure

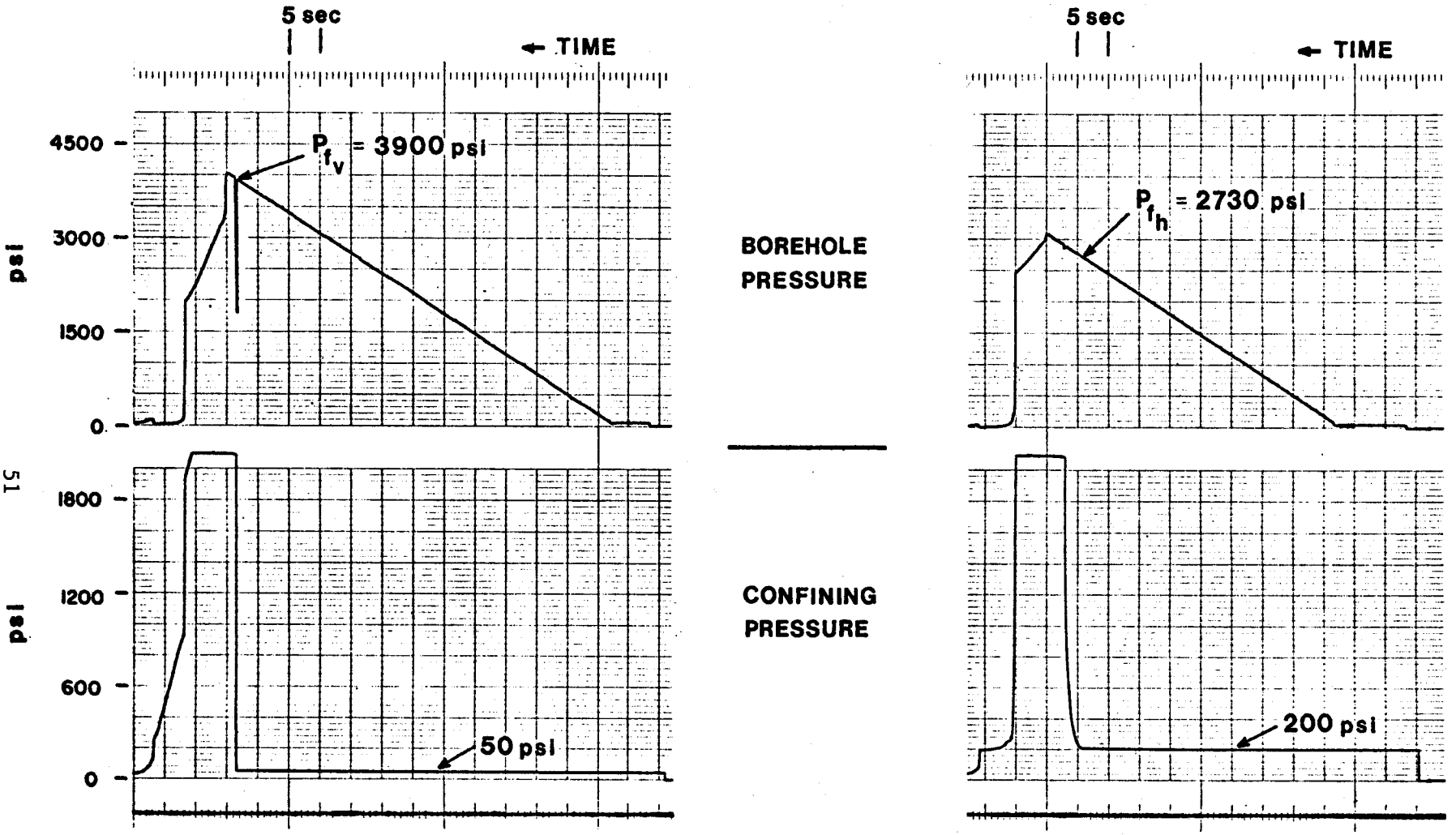

Figure 18. Pressure-time records for typical hydraulic fracturing tests. a) Vertical fracture record. b) Horizontal fracture record for intact sample. (Chart speed - 1mm per second)

All vertical fractures were well defined planes which aligned themselves parallel to the borehole axis. These planes extended in both directions from the borehole (Fig. 19). In all but two samples the halves of the failure plane on either side of the borehole were 180° apart (Fig. 20). The two exceptions showed angles of 145° and 120° between their fracture plane directions.

Arbitrarily defining one of the orientation directions established for the quarry block as 0 degrees, vertical fracture plane directions were recorded. A frequency diagram of the angular orientation of these planes (Fig. 21) clearly shows that a generally preferred fracture direction exists. Practically all of the failure planes were directed between 0 and 90 degrees. Fracture planes extending in two different directions from the borehole were both plotted, each representing only one-half of a sample.

Intact specimens that failed horizontally showed pressure records very similar to vertically fractured samples (Fig. 18b). Some slight increase in confining pressure was observed just before distinct breakdown occurred. Breakdown pressure in this case was taken at the point where the confining pressure began to increase very rapidly. Figure 22 shows typical horizontal fractures.

In the case of horizontal fracturing in prefractured samples, breakdown pressure could not be clearly defined. In the majority of cases, leak-off began to occur through preexisting bedding plane fractures soon after the borehole pressure reached the vertical stress σ_z. This fluid

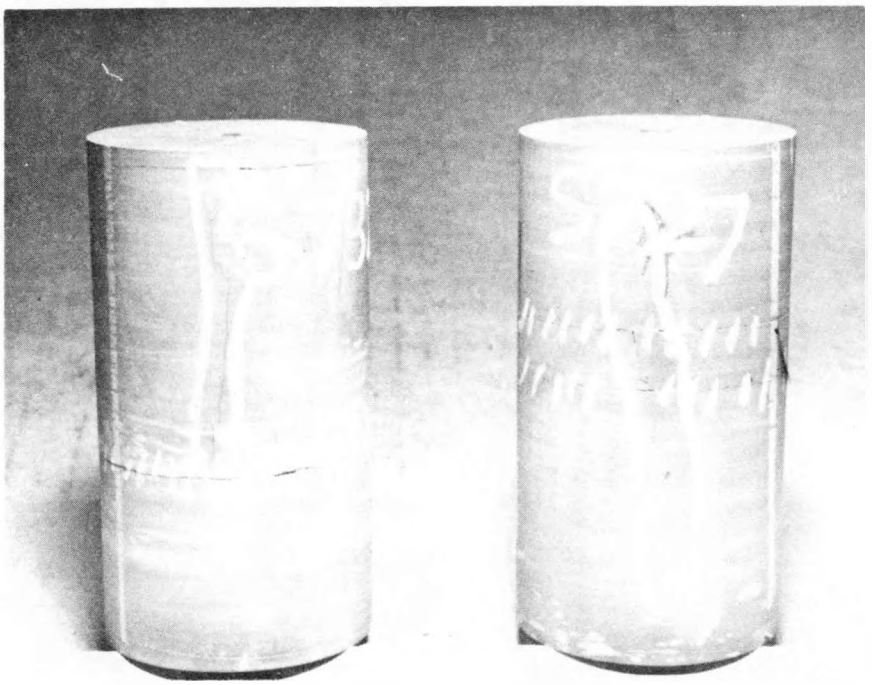

Figure 19. Typical vertical fractures for nipple packer tests. Fracture planes are outlined by solid lines. Pre-fractures shown by hachures.

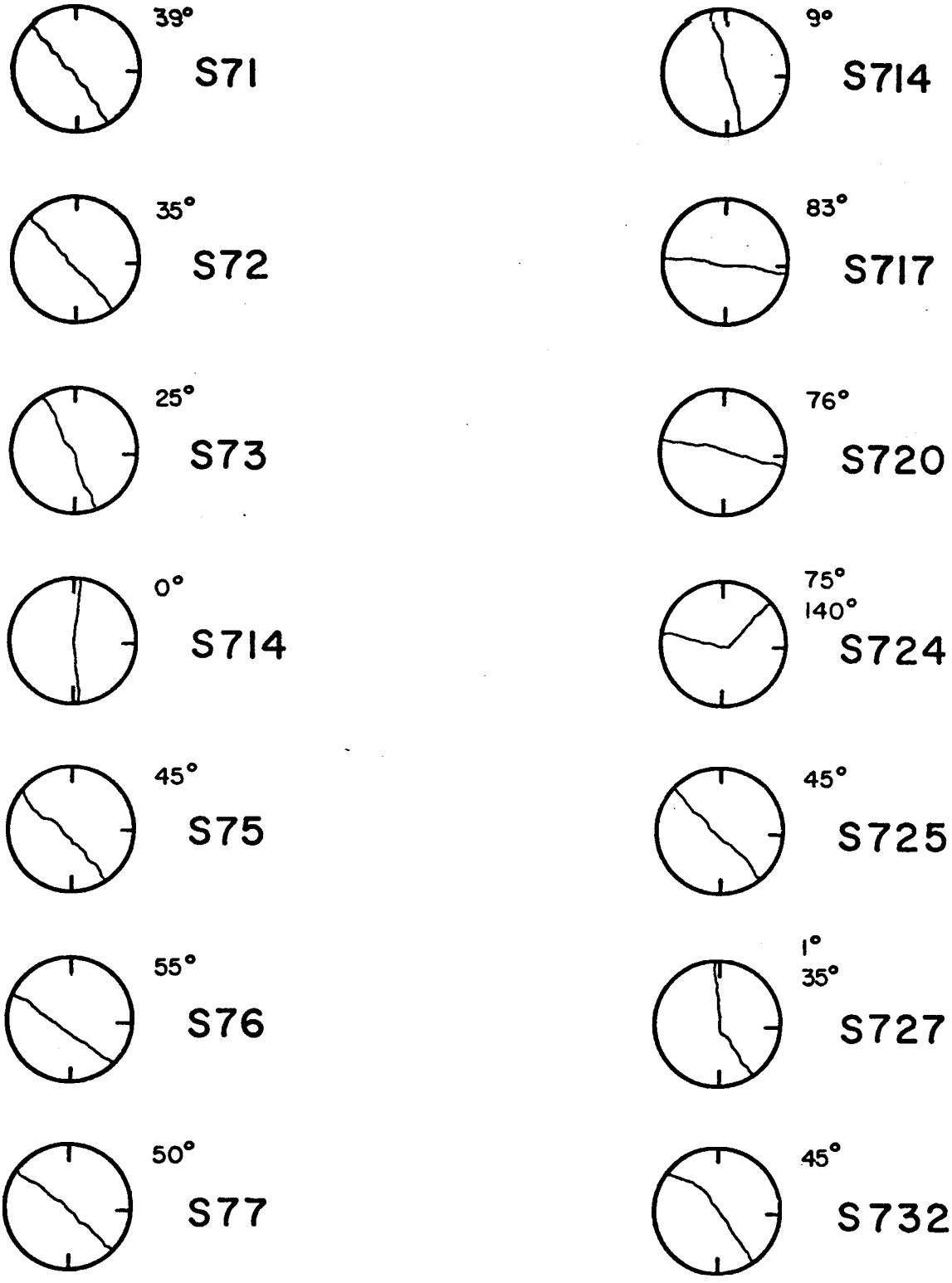

Figure 20. Vertical hydraulic fracture plane direction relative to orientation marks for nipple packer tests on Antrim Shale (as viewed from top of sample). Directions measured counter-clockwise from orientation mark pointing to top of page.

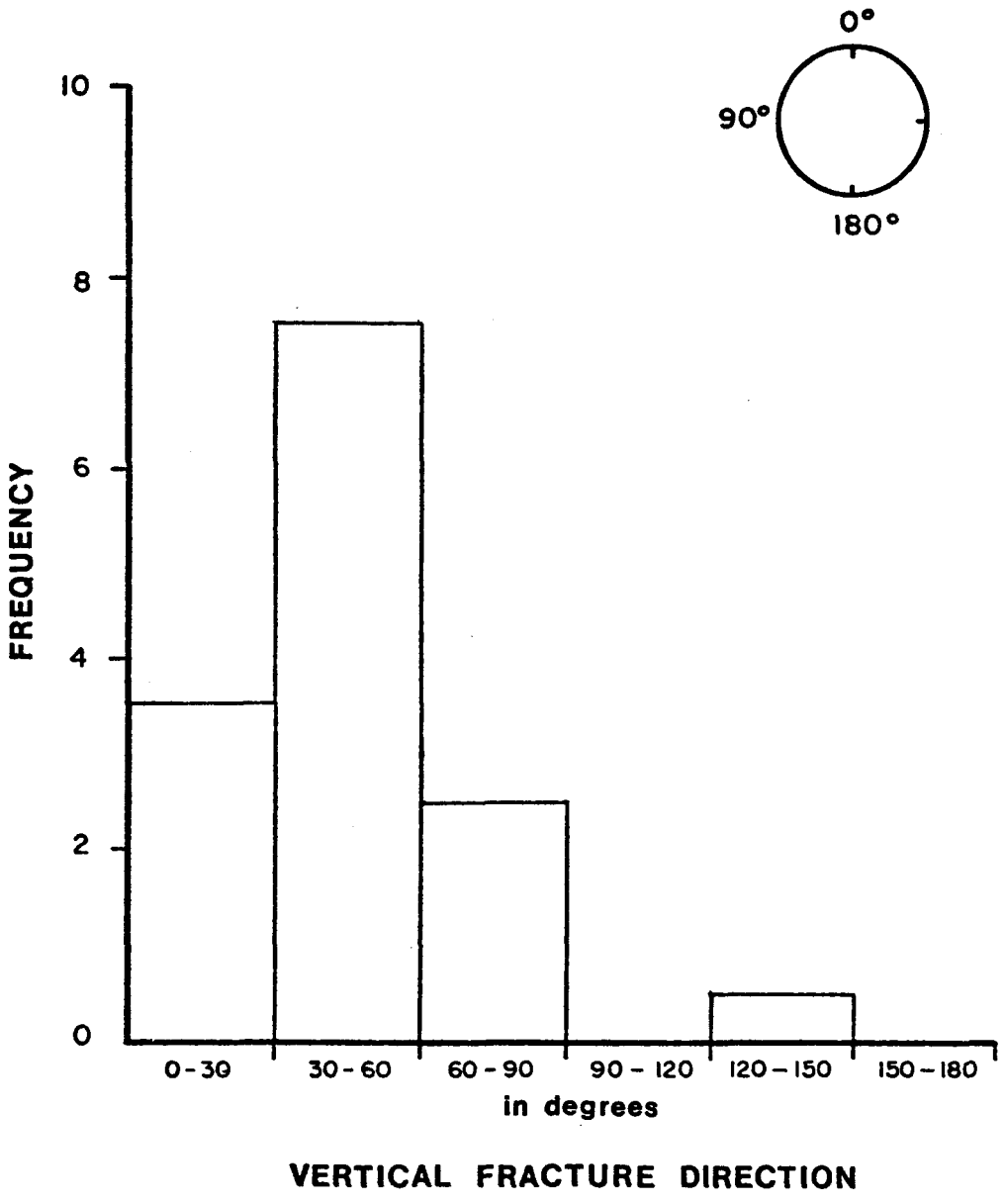

Figure 21. Frequency diagram for vertical fracture directions from nipple packer tests (Paxton quarry block 7). Inset shows sample top with orienting marks and directional convention assumed.

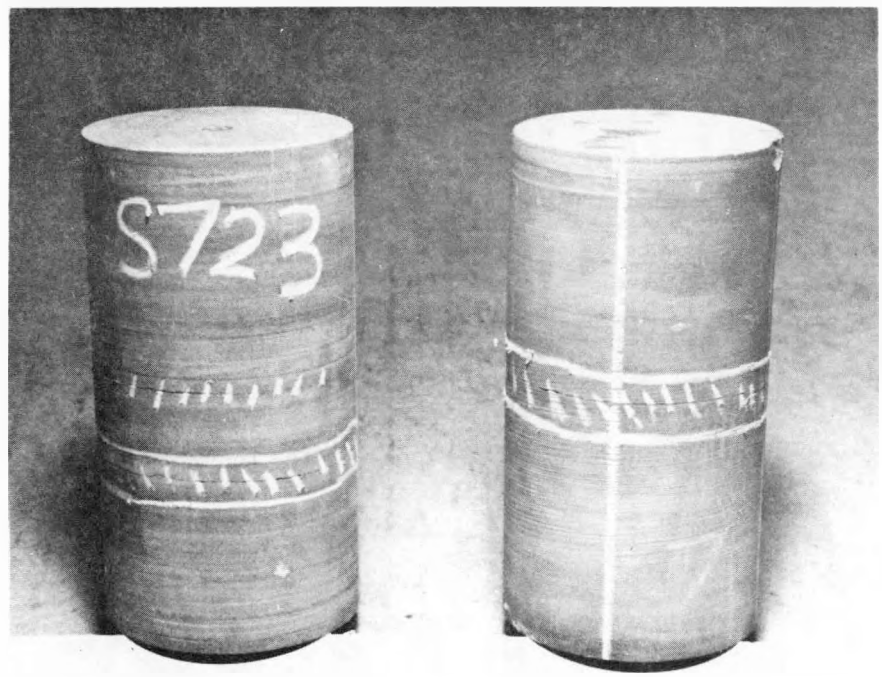

Figure 22. Typical horizontal fractures for nipple packer tests. Fracture planes are outlined by solid lines. Pre-fractures shown by hachures.

made contact with the triaxial membrane causing the confining pressure to gradually increase (Fig. 23). At some point during pressurization the flow through prefractures became totally unrestricted and the confining pressure quickly caught up to the borehole pressure. It was decided that failure would be defined at a point where confining pressure was some given percent above its original value. Prefractured specimens were assumed to have zero tensile strength perpendicular to bedding (T_1). Since the borehole pressure acts directly on the borehole bottom, failure in these specimens should take place at approximately 1500 psi, the applied axial stress. Each of the pressure records showed that when the confining pressure was 25 percent above its initial value a borehole pressure near 1500 psi was indicated. Thus, for horizontally fractured samples showing leak-off, failure pressure was taken at the point where confining pressure was 25 percent in excess of its original value. As an example, Figure 23 shows a specimen with an initial confining pressure of 150 psi. When the confining pressure reached 190 psi (25 percent above its initial value) the corresponding borehole pressure (1500 psi) was recorded as the failure pressure.

The results of Tables 1 and 2 are shown graphically in Figure 24. A linear regression program was run on the vertical failure data. Although the linear regression line shows the same trend suggested by equations (3.43) and (3.45) a correlation coefficient of only 0.34 was indicated. It is believed, however, that this increasing trend is present. Haimson's (1974) laboratory hydraulic fracturing experiments

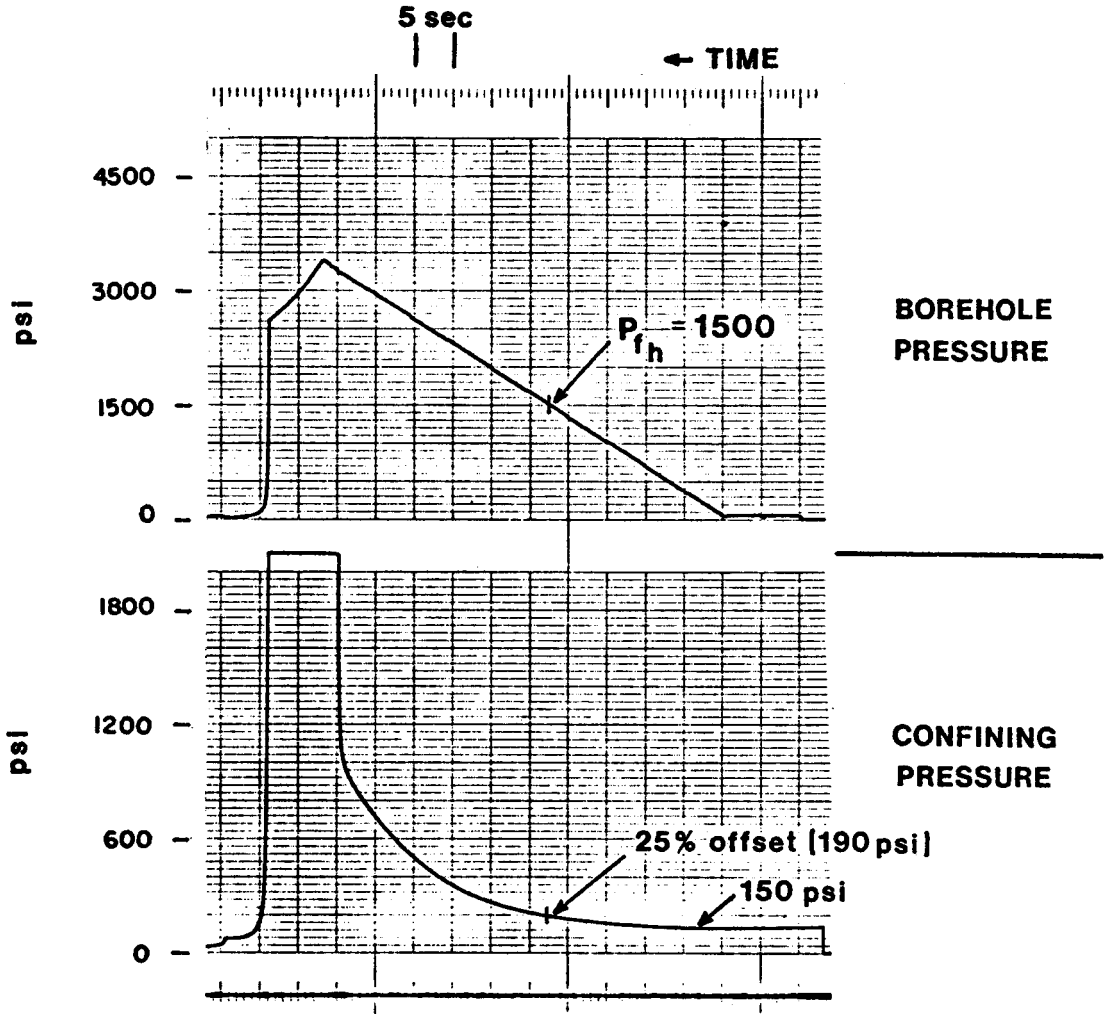

Figure 23. Pressure-time record for typical hydraulic fracturing test on a prefractured sample yielding a horizontal fracture. (Chart speed - 1mm per second)

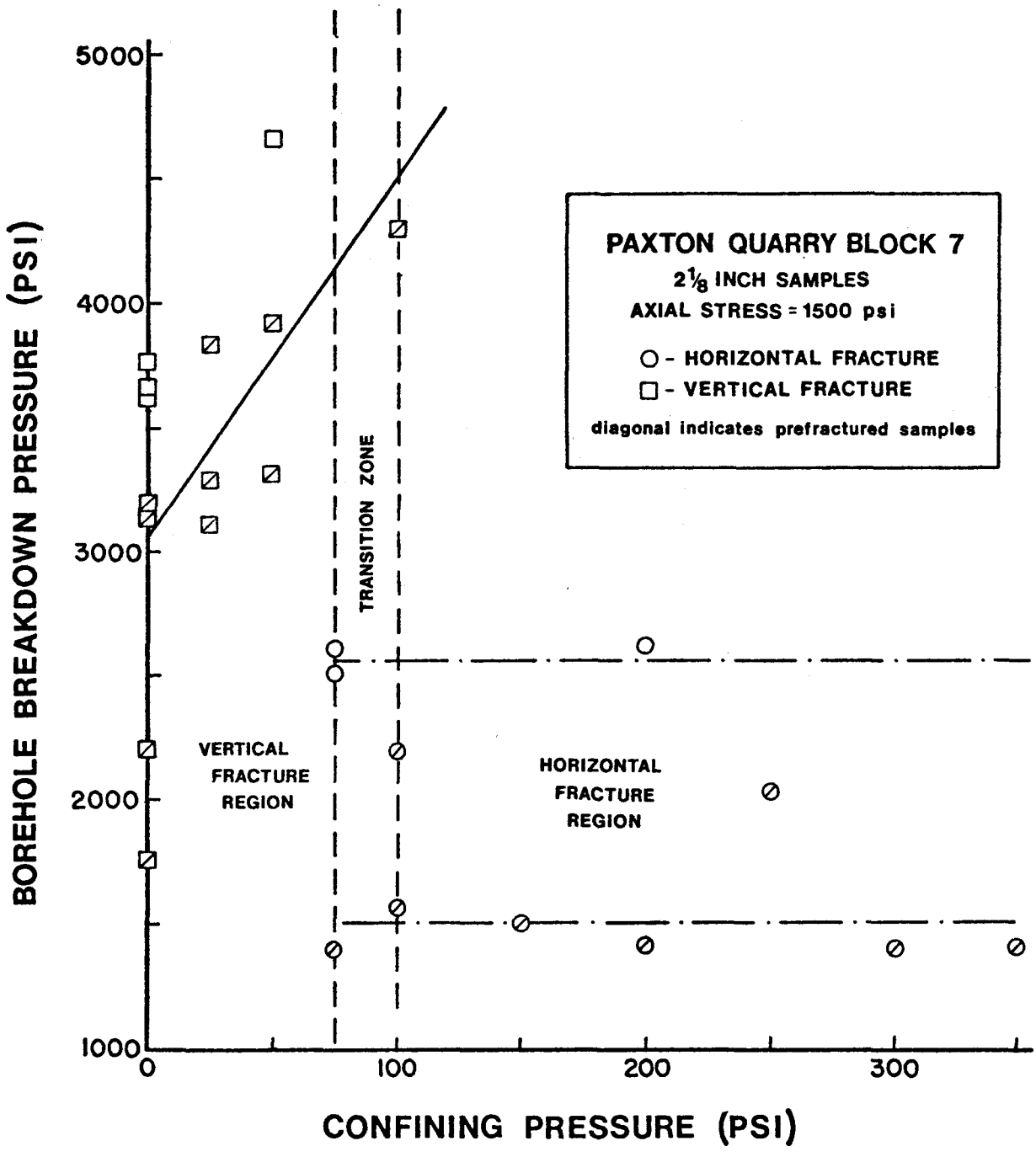

Figure 24. Hydraulic fracturing results for nipple packer tests on Antrim Shale.

on quartzite (some of which was prefractured) also shows this increasing trend.

The theoretical development for horizontal fractures indicates that for the case of equal horizontal stresses ($P_1 = P_2$) and a constant vertical stress, breakdown pressures should be independent of the confining pressure. Any variation in failure pressure then, can be attributed to variations in the tensile strength T_1. Obviously, prefractured samples have very low values of T_1, if not zero, while intact specimens have substantially higher tensile strengths. The data indicate that horizontal breakdown pressures for prefractured specimens do, in fact, show no dependence on confining pressure for the range of pressures used here. These failure pressures also group around 1500 psi as expected. A horizontal line through these points (at a breakdown pressure of 1500 psi) in Figure 24 defines the lower limit for horizontal hydraulic fracturing failure pressures.

Fully intact specimens failed horizontally at pressures between 2500 and 2700 psi. This suggests a maximum tensile strength value perpendicular to bedding of 1000 to 1200 psi for the quarry blcok. The proposed upper limit for horizontal failure pressures is drawn through these points at a borehole pressure of 2700 psi. It is possible for some specimens to fail at pressures between these two bounds; samples plotting in this region possess a tensile strength greater than prefractured samples but less than the maximum possible.

Results of Miniature Straddle Packer Investigation

Packer Operation

As was noted in the previous chapter, considerable difficulty was encountered in making the miniature packer leak-free. Once the proper adhesive and mounting technique had been discovered, the packer was tested to determine its sealing ability. It was initially felt that a certain minimum packer set-pressure would be required to hold back a given borehole pressure. A packer failure curve (plot of various packer set-pressures versus their corresponding extrusion pressures) would allow the choice of a reasonable set-pressure for a given anticipated breakdown pressure. This would minimize the possibility of premature borehole breakdown during setting of the packer.

The packer was tested in unconfined plexiglass specimens with the same computer program used for rock samples. This allowed direct visual observation of the packer's behavior during testing.

Once the plexiglass sample was axially loaded, the inflatable packer elements were pressurized and could be seen to expand until they made full contact with the borehole wall (Fig. 25). The rubber membranes were inflated to their full set-pressure and then the sealed-off interval between them was gradually pressurized. The air previously occupying this annulus became compressed until only a small bubble at the top of the pressurizing interval remained. When the borehole pressure became equal to the packer set-pressure, borehole fluid began to slip past part of the inflatable sleeve. This, in effect, began to increase the

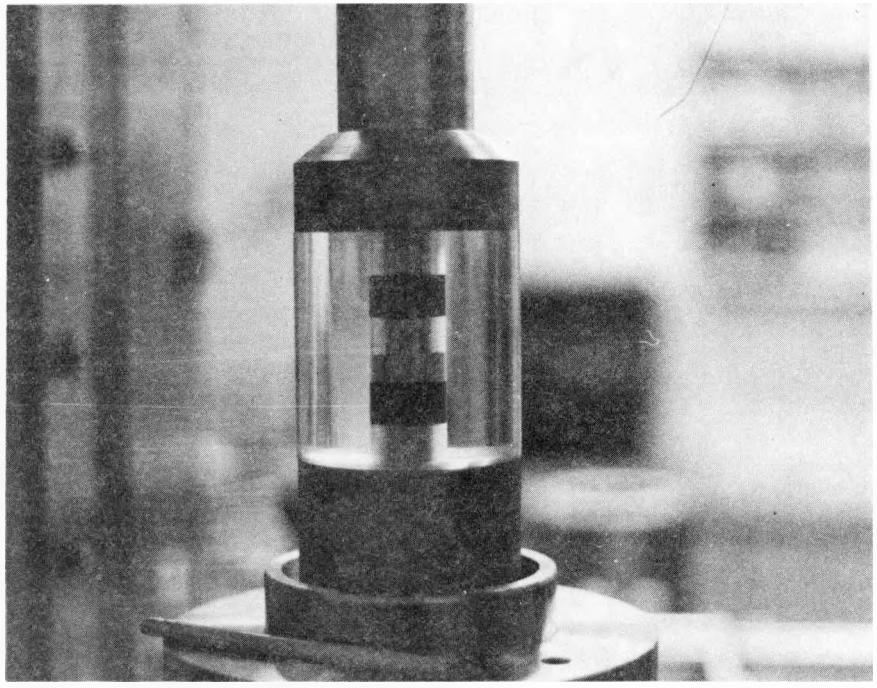

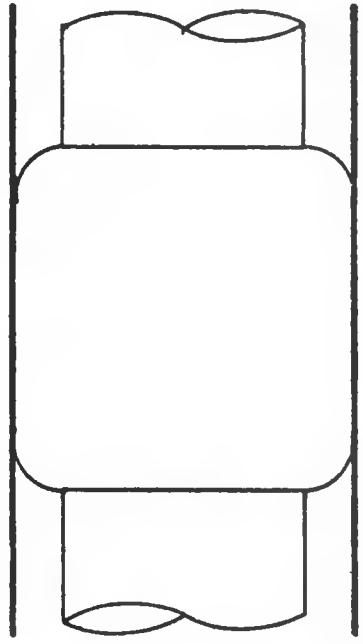

Figure 25. Miniature straddle packer "set" in plexiglass sample, pressurizing interval is being filled with oil.

length of the pressurized interval. Since the packer setting fluid has a fixed volume and is incompressible, the borehole fluid acting on the rubber membranes caused the packer pressure to increase. From this point on, the packer pressure remained identically equal to the borehole pressure. Continued pressurization of the borehole caused the inner rubber-borehole contact point to migrate away from the center of the pressurized interval (Fig. 26).

At this stage, the borehole pressure may continue to push back the rubber membranes until leakage occurs. Rubber-borehole contact will always be present, however, since the packer pressure and borehole pressure are equal. This was the case in many of the first plexiglass tests. Increasing the initial packer set-pressure was not a solution to this problem because once the borehole pressure reaches the packer set-pressure, the two remain equal throughout the remainder of the test.

After repeated use, rubber membranes were found to become more pliable. Pressurization beyond the stage shown in Figure 26 with previously used packer elements caused the membranes to begin to act like a set of O-rings. The rubber near the outer ends of the packer (away from the center of the pressurized interval) physically plugged the annulus and even began to extrude at higher pressures (Fig. 27). The length of the pressurized interval then became equal to the distance between the outer ends of the inflatable packer elements. This type of packer behavior was found to occur when using previously pressurized membranes at all packer set-

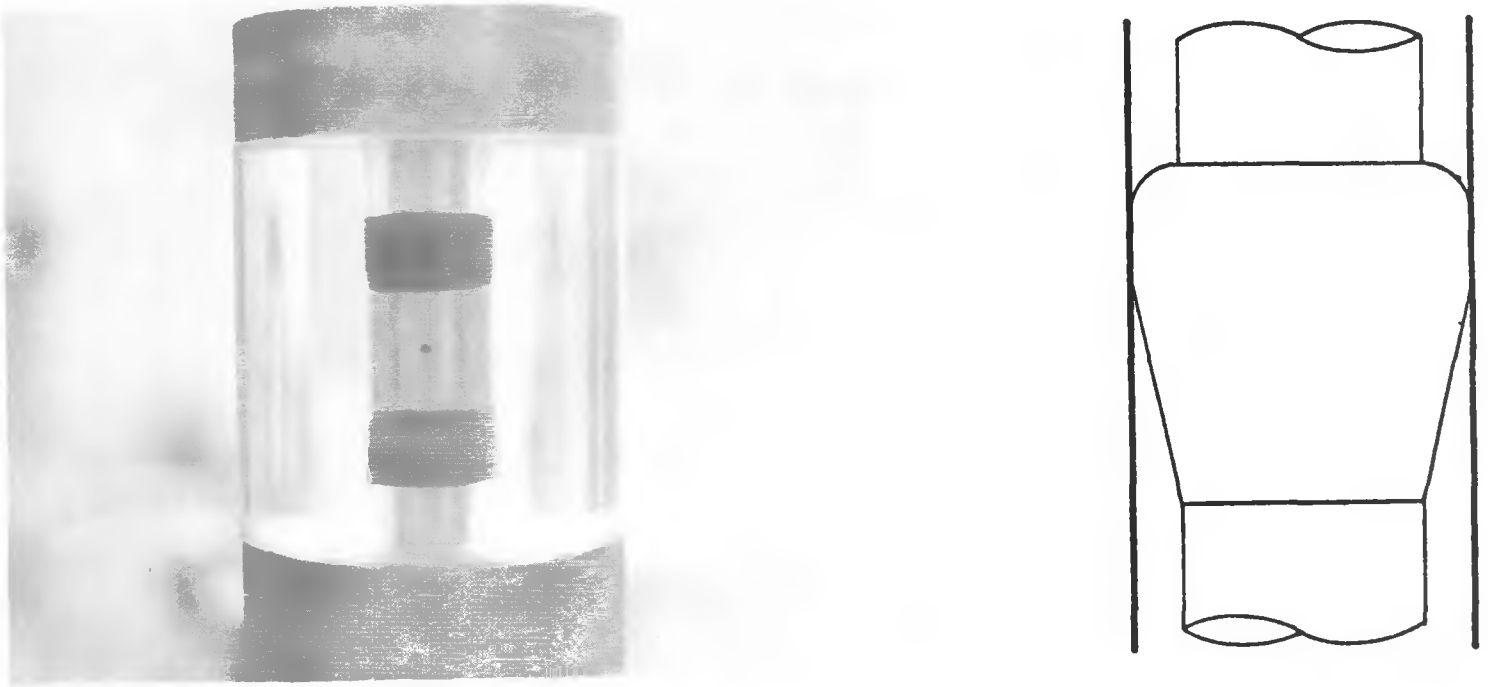

Figure 26. Miniature straddle packer shortly after borehole pressurization begins. Packer elements beginning to be pushed away from plexiglass wall by pressurizing fluid.

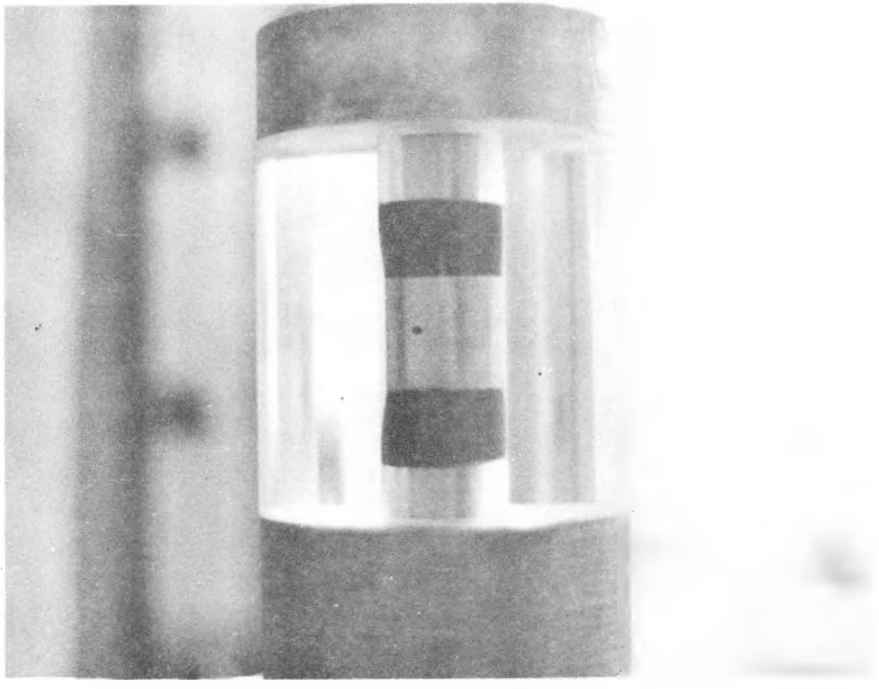

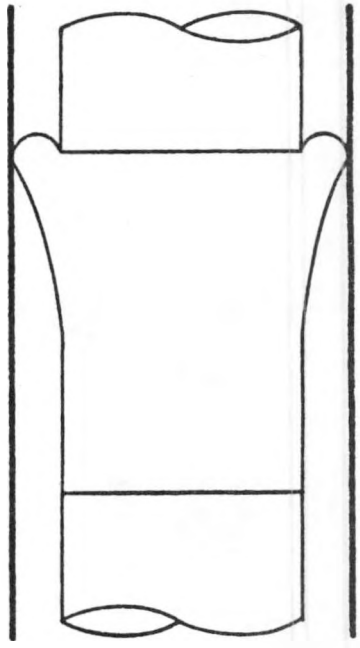

Figure 27. Miniature straddle packer after it has formed a static physical plug in the annulus. Packer elements are beginning to extrude.

pressures above 300 psi. Apparently, a pressure of 300 psi is needed to insure the rubber membranes create a static physical plug in the annulus.

Hydraulic Fracturing Results

a) Paxton Quarry Block Samples.

All 3-1/2 inch diameter quarry block samples were tested with 1500 psi axial stress and an initial packer set-pressure of 300 psi. Unconfined tests were run on five samples to determine their in-bedding-plane tensile strength. With the exception of one anomalously high value the breakdown pressures indicate a tensile strength between 1650 and 3000 psi (Table 3), the average of all five being 2690 psi.

The remaining samples were tested at confining pressures up to 300 psi. The results of these tests are listed in Table 3. As with the nipple packer tests, distinct vertical and horizontal fracture regions were defined with a transition zone occupying the area between these two regions (Fig. 28).

Pressure-time records for the straddle packer tests which resulted in vertical fractures were very similar to those obtained with the nipple packer. A very clear breakdown was observed for vertical failures. Samples displaying horizontal fractures did not show clear initiation points despite the fact that none contained significant prefractures. Pressure-time records for horizontal fractures were similar to that shown in Figure 23. In order to compare the results obtained for the two different packer types, a 25 percent increase in confining pressure (over its initial value) was again used to mark the point of horizontal failure.

TABLE 3

Hydraulic Fracturing Results for 3-1/2 inch Antrim Shale Cores from Paxton Quarry Block 8

Sample	Axial Stress (psi)	Confining Pressure (psi)	Breakdown Pressure (psi)	Fracture Orientation
8B 12	1500	0	2160	vertical
8B 15	1500	0	2885	vertical
8B 18	1500	0	2700	vertical**
8B 20	1500	0	4030	vertical
8B 6	1500	0	1670	vertical
8B 9	1500	13	1830	vertical
8B 27	1500	20	2040	vertical
8B 11	1500	25	3180	vertical
8B 16*	1500	25	2190	horizontal
8B 19*	1500	25	1730	horizontal
8B 24	1500	25	1700	vertical
8B 25*	1500	25	2250	horizontal
8B 22	1500	50	1575	vertical
8B 26*	1500	75	2110	horizontal
8B 8*	1500	100	2000	horizontal
8B 14	1500	100	1640	vertical
8B 23*	1500	150	2060	horizontal
8B 7	1500	200	2200	horizontal
8B 17*	1500	200	1830	horizontal
8B 3*	1500	300	1790	horizontal
8B 13*	1500	300	2070	horizontal

*Indicates breakdown pressure was defined by 25% increase in confining pressure.

**Failure plane was slightly inclined.

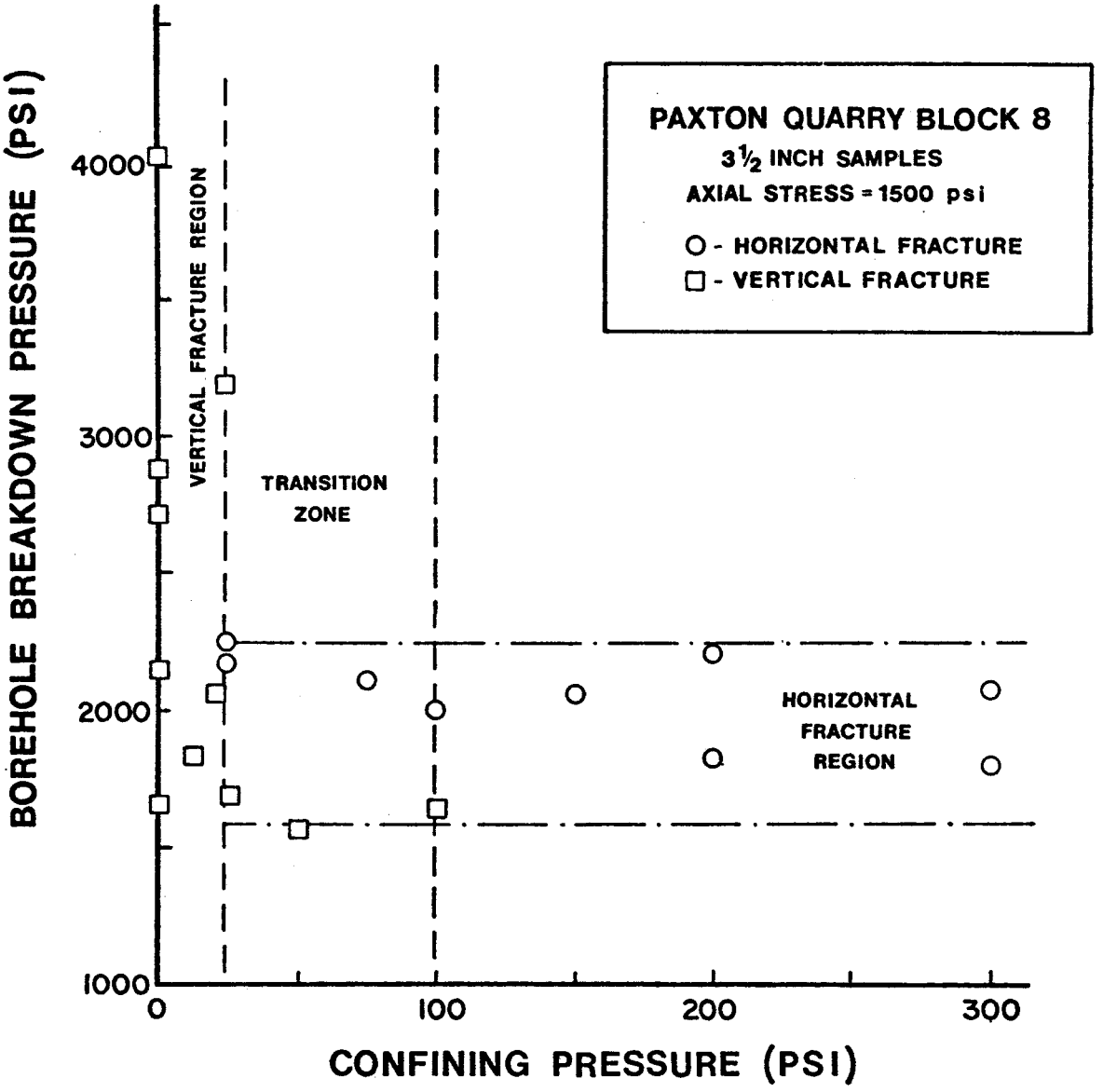

Figure 28. Hydraulic fracturing results for miniature straddle packer tests on Antrim Shale.

Vertical failure pressures did not show the trend predicted by equations (3.43) and (3.45). Contrary to the results obtained with the nipple packer, vertical failure pressures in the transition zone were consistently lower than horizontal breakdown pressures. Vertical fractures were planar surfaces extending away from the borehole on both sides of the sample (Fig. 29). Three samples showed fracture extension to the external cylindrical wall on only one side of the borehole. Further examination of these specimens (by cutting them in half) showed that the fracture plane was present on the opposite side of the borehole, but did not extend to the outside wall.

Vertical fracture directions were recorded (Fig. 30) and plotted on a frequency diagram as before (Fig. 31). A very distinct preferred direction is indicated. Relative to the arbitrary 0 degree mark, the majority of samples show failure planes directed between 60 and 90 degrees. A secondary preferred direction, 90 degrees away, may be indicated by the samples showing fractures between 150 and 180 degrees.

Horizontal fracture planes formed parallel to bedding in all cases (Fig. 32). The majority of horizontal fractures were also located near the end of the sealed-off interval, as predicted by theory.

The horizontal failure data show little or no dependence on the confining pressure. The upper bound for the horizontal fracture region can be placed at a breakdown pressure of 2250 psi. Since none of the 3-1/2 inch samples contained significant prefractures, a lower limit for the horizontal failure region cannot be verified. Equation (3.44),

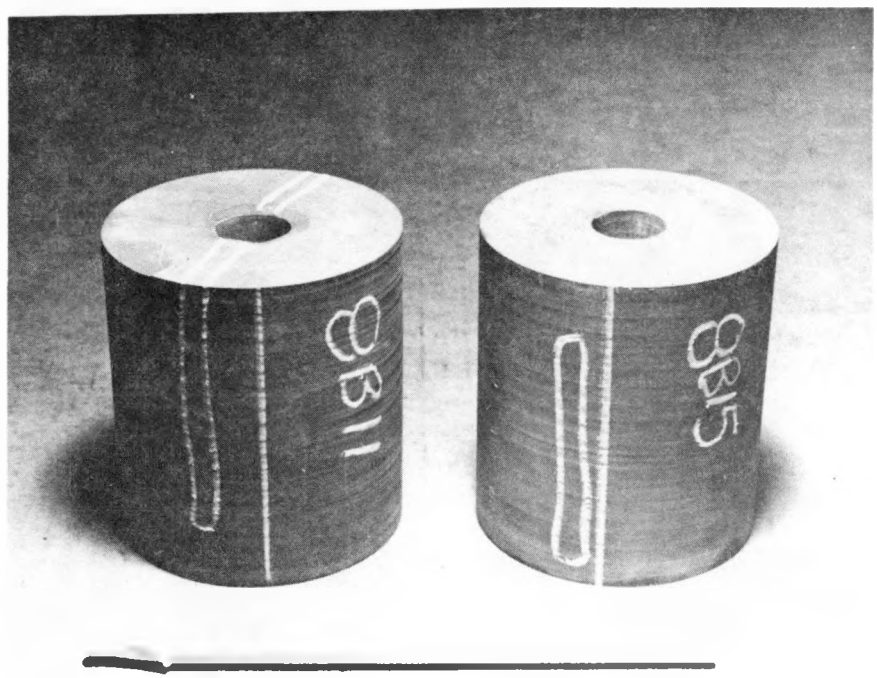

Figure 29. Typical vertical fractures for miniature straddle packer tests. Fracture planes are outlined by solid lines. Prefractures shown by hachures.

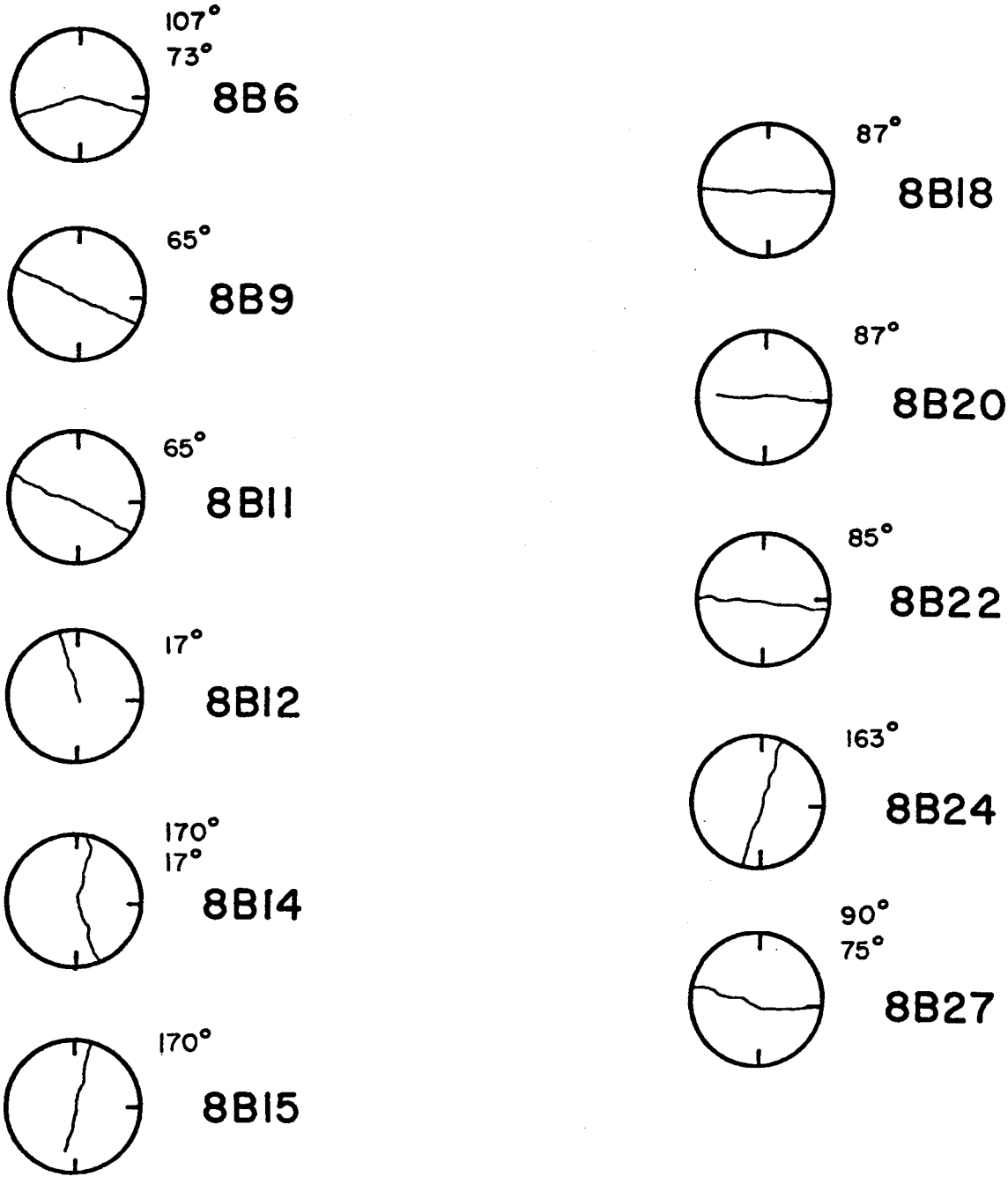

Figure 30. Vertical hydraulic fracture plane directions relative to orientation marks for straddle packer tests on Antrim Shale (as viewed from top of sample). Directions measured counterclockwise from orientation mark pointing to top of page.

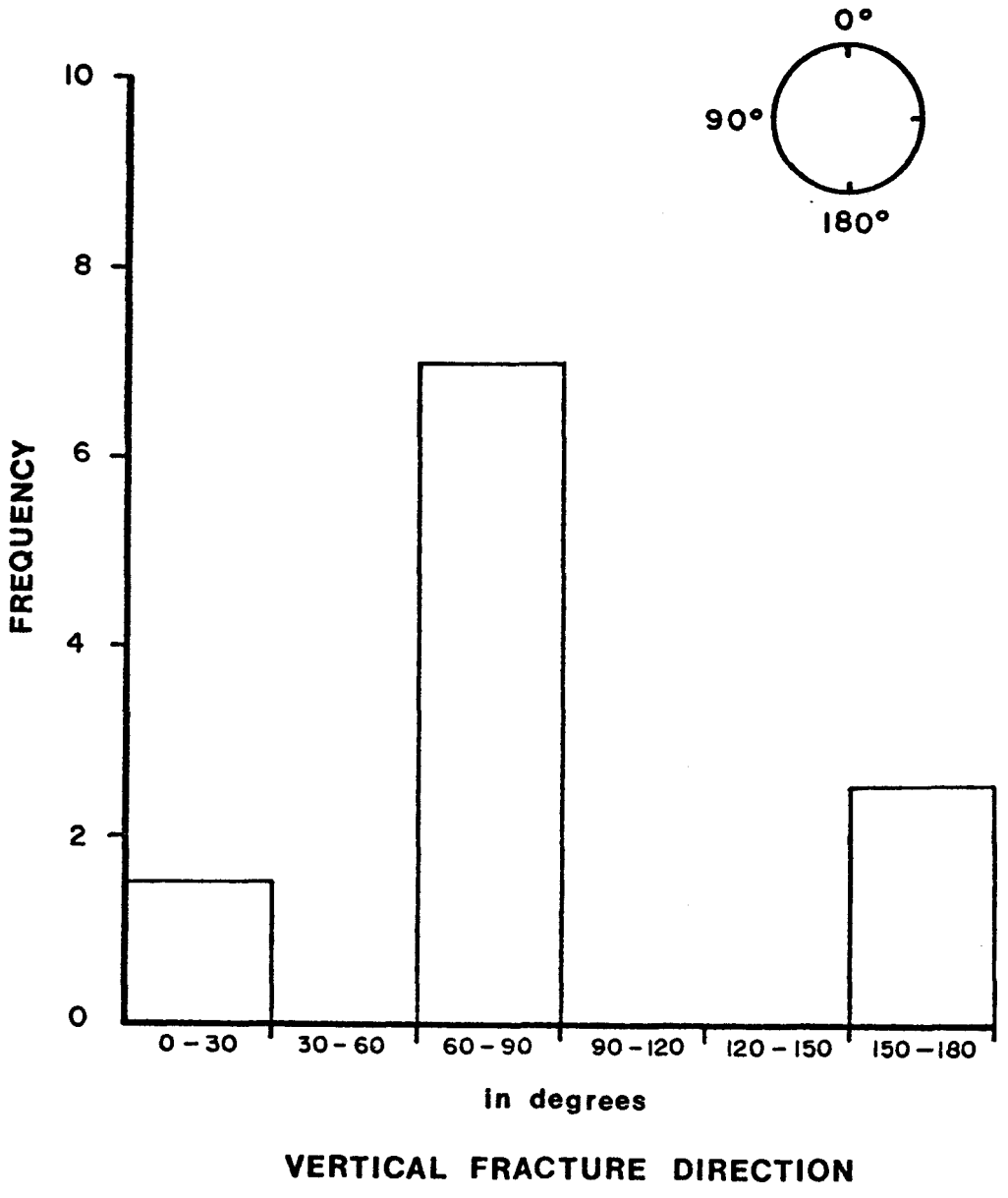

Figure 31. Frequency diagram for vertical fracture directions from miniature straddle packer tests (Paxton quarry block 8). Inset shows sample top with orienting marks and directional convention assumed.

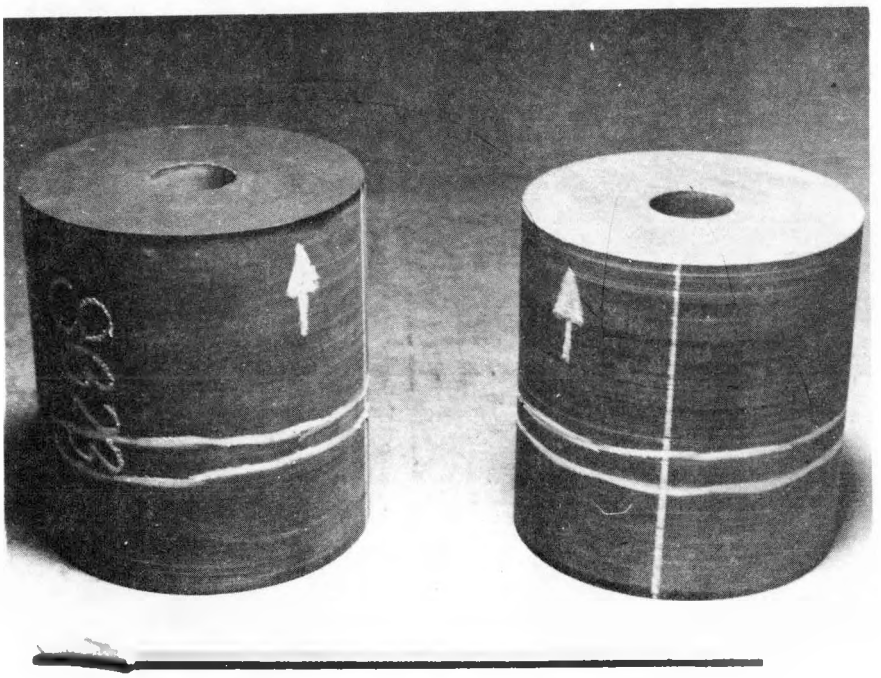

Figure 32. Typical horizontal fractures for miniature straddle packer tests. Fracture planes are outlined by solid lines. Prefractures shown by hachures.

however, suggests it should be placed at a borehole pressure level of 1590 psi. This results in a tensile strength value of 660 psi in a direction perpendicular to bedding.

b) Dow/ERDA 100 samples

Cores taken directly from Dow Chemical's Dow/ERDA well 100 were tested unconfined to determine their in-bedding-plane tensile strength. The results of this test are presented in Appendix II.

DISCUSSION

Experimental Hydraulic Fracturing

In Chapter 3, theoretical breakdown pressures for an isotropic, homogeneous, and linearly elastic material were plotted for various confining pressure values at a constant axial stress (Fig. 4 and 5). It was suggested that transition from vertical to horizontal fractures took place when the two failure curves crossed. At confining pressures less than that at the transition point, vertical breakdown pressures were lower than horizontal ones. Thus it was assumed that vertical fractures would occur in all tests at these lower confining pressures. Confining pressures higher than that at the transition point would result in horizontal fractures.

The experimental data, although for a material not meeting the theoretical assumptions (especially in the case of prefractured samples), show a transition from vertical to horizontal fractures with increasing confining pressures, as predicted by theory. It is clear from Figures

24 and 28, however, that the lower predicted breakdown pressure does not determine which type of failure takes place. In Figure 24, the best fit line through vertical fracture points does not even come close to intersecting the horizontal fracture region. Failure plane orientation is, though, a function of the applied confining pressure (for the case of constant axial stress). Complete transition from vertical to horizontal fractures took place in the Antrim Shale at a confining pressure of 100 psi (for 1500 psi axial stress).

Vertical plane directions show that some anisotropy is present in the plane of bedding. Both nipple packer and straddle packer tests indicated the presence of a preferred fracture direction. Since the quarry blocks were not oriented relative to true compass directions, no comparison is possible between the two blocks. It is believed that the preferred fracture directions would coincide between the two blocks if they were oriented relative to each other.

The experimental breakdown data for horizontal fractures, obtained with both types of packers, agrees very well with theoretical predictions. That is, above a certain critical confining pressure, a band of breakdown pressures plot which show no dependence on confining pressure. The upper and lower limits of this band describe failure pressures for fully intact and horizontally prefractured samples, respectively. The difference between the upper and lower limits yields the hydraulic fracturing tensile strength T_1.

A finite transition zone divides the two fracture orientation regions. The presence of this transition zone is probably due to slight variations in both rock properties and testing techniques. Both nipple packer and straddle packer testing placed the horizontal fracture - transition zone boundary at a confining pressure of 100 psi. The vertical fracture - transition zone boundary differs for the two packer types, being 25 psi for the straddle packer and 75 psi for the nipple packer. This difference may be the result of sample geometry. The nipple packer tests used samples with a length to diameter ratio near two. The straddle packer tests however had an L/D ratio near one. (Physical constraints of tri-axial cell dimensions and maximum recoverable sample length forced this low ratio.) The length to diameter ratio for the pressurization interval also varied between the two phases of testing being larger for the nipple packer tests.

The values of T_1 and T_2 obtained from the miniature straddle packer data are lower than those from nipple packer tests. This difference is most likely due to sample size effects. Haimson and Fairhurst (1969) have shown that as the outer to inner diameter ratio decreases, breakdown pressures also decline.

Straddle Packer Operation

To this author's knowledge, information concerning the sealing mechanics of an in-field straddle packer has not been published. Therefore, it is difficult to know how realistic the miniature packer used in this study behaved.

Packer elements on full size straddle packers obviously are much more rigid than those used here. Commonly the elements are made of a very hard compound and often steel reinforcing is molded into the rubber. It is likely that this type of packer element would not assume the shape depicted in Figure 27. This shape, however, was found in this study to be necessary in order to hold back the borehole fluid.

Little field or laboratory information is available regarding packer set-pressures. Abou-Sayed et al. (1978) indicate that at a depth of 2745 feet a packer set-pressure of 1520 psi was adequate to hold back a borehole pressure of 2930 psi before the formation was hydraulically fractured. It would seem reasonable to assume that the packer elements must have behaved somewhat similar to those described here to facilitate this.

In another paper indicating packer setting strategy, Bredehoeft et al. (1976) indicate that the packer elements were inflated to a pressure 100 psi above the expected breakdown pressure. If their estimate of the breakdown pressure was sufficiently accurate (within 100 psi of the true failure pressure), this could only lead to premature breakdown of the borehole during packer setting. (Incidentally, this may explain the extremely low tensile strength values they recorded.)

The packer behavior described in this study indicates that a high (near breakdown pressure) packer set-pressure is not necessarily required to insure the sealing ability of a straddle packer.

CONCLUSIONS

Regarding laboratory hydraulic fracturing in the transversely isotropic Antrim Shale, the following conclusions can be made:

1. The orientation of failure planes generated by hydraulic fracturing is governed not only by the prevailing stress state but also by the rock properties.
2. Distinct vertical and horizontal fracture regions could be defined on plots showing borehole breakdown pressure versus confining pressure. A finite transition zone was defined for the region where both vertical and horizontal fractures occurred. The presence of this region is probably due to slight variations in rock properties from sample to sample.
3. For the Antrim Shale from Paxton clay quarry, all tests with confining pressures in excess of 100 psi (axial stress constant at 1500 psi) showed horizontal fractures.
4. Despite the fact that the Antrim Shale specimens in this study did not fit the assumptions used to develop theoretical fracturing criterion, vertical and horizontal failure pressure trends generated by laboratory testing agree quite well with theoretically predicted trends.
5. Hydraulic fracturing tensile strengths in the bedding plane (T_2) varied from 2690 to 3660 psi. Tensile strengths perpendicular to bedding (T_1) ranged from 0 (prefractured speciments) to 1200 psi.

6. The hydraulic fracturing tensile strength varies with sample geometry (outer to inner diameter ratio).
7. Vertical failure planes showed a preferred direction indicating some degree of anisotropy in the bedding plane.
8. The hydraulic fracturing tensile strength in the bedding plane of Dow/ERDA well 100 cores increases with depth from the top of the formation (1210 feet) to a depth of 1375 feet. Immediately below this level it shows a sudden drop. This abrupt change can be related to a lithofacies change.
9. Orientation grooves on the Dow/ERDA well 100 cores altered hydraulic fracture plane directions. The failure planes changed direction during propagation to meet the groove at the external core wall.
10. It appears that in tectonically relaxed areas and at shallow depths, the possibility for horizontal fractures to be consistently produced in strongly anisotropic rock does exist.

Concerning packer operation and utilization, it can be concluded that:

1. Both the nipple packer (O-ring - borehole contact) and miniature straddle packer (inflatable membrane - borehole contact) were capable of holding back significant borehole pressures (up to 5000 psi).

2. Results from miniature straddle packer and nipple packer tests were quite similar. Vertical fracturing pressures, however, from straddle packer tests did not agree with nipple packer tests (perhaps the result of L/D ratios).

3. Soft rubber (60 - 70 durometer) proved to work best for both the nipple packer (O-rings) and miniature straddle packer (inflatable packer elements). In both cases the rubber formed a physical plug in the annulus between the packer and borehole wall. For the straddle packer, this plug allowed a large pressure to be applied in the borehole without a high packer set-pressure.

4. A minimum packer set-pressure of 300 psi was found to be necessary for the inflatable rubber membranes to form the plug mentioned in item 3.

5. Nipple packer sealing failure (when the type of behavior mentioned in item 3 occurred) took place when the O-rings extruded. In miniature straddle packer tests extrusion could not take place since the packer elements were too large to be forced into the annulus. The effort of the borehole pressure to cause extrusion, however, resulted in numerous failures of the epoxied contacts between the packer and the inflatable membranes. In holding the rubber membranes to the packer, Scotch Weld Structural Adhesive 1838 was found to be stronger than any other epoxy or adhesive used.

RECOMMENDATIONS FOR FUTURE STUDY

This study, although by no means definitive, has revealed the real possibility for generation of horizontal hydraulic fractures. Continued laboratory and field studies of hydraulic fracturing in distinctly transversely isotropic rocks will lead to an enhanced understanding of the conditions under which horizontal fractures take place.

The following studies should be added to this work to provide a broader and more realistic picture of hydraulic fracturing in transversely isotropic rocks:

1. Complete stress field

The stress state of axial and confining stresses should be expanded to include an axial and two horizontal stresses. This will require some modifications of equipment, however, a much more realistic duplication of field situations will result.

2. Variation of all stresses

The present study utilized only one axial stress for all tests. Tests utilizing different axial loads will yield similar transition points between vertical and horizontal fractures. A plot of axial stress versus confining pressure showing transition points will indicate the vertical stress' effect on fracture orientation. Following development of recommendation 1 above, a three-dimensional plot will show the complete transition surface.

3. Notched samples

It would be relatively simple to prepare samples with one or a series of notches along the borehole wall in the area to be hydraulically fractured. The transition zone may be moved due to these notches.

4. Other borehole wall modifications

Fracture orientation could be studied in samples that were partially retorted in the pressurizing interval or that had cased and perforated boreholes.

5. Field packer operation

A laboratory study of the sealing mechanics of a field packer should be performed. Different packer element designs and compounds should be studied by observing their behavior during typical operation. Valuable information concerning required packer set-pressures and expected sealing abilities could be generated.

6. Photoelastic studies

Using a photoelastic plexiglass, the changes in the stress state surrounding the borehole during external and internal pressurization may be studied using a polariscope. A series of photographs during the hydraulic fracturing operation may allow the development of a model which improves on Kehle's. Particularly, the effect of the packer elements on the stresses at the borehole is of interest. (Laminated plexiglass samples may be formed by glueing together slices of plexiglass to represent a transversely isotropic material.)

BIBLIOGRAPHY

Abou-Sayed, A.S., Brechtel, C.E., and Clifton, R.J., 1978. In Situ Stress Determination by Hydrofracturing: A Fracture Mechanics Approach, Jour. of Geophys. Res., Vol. 83, pp. 2851 - 2862.

Bennett, G.H., 1978. Sedimentology of the Antrim Shale from Five Drill Sites in the Michigan Basin, M.S. Thesis, Michigan Technological University, Houghton, Michigan, 75 p.

Biot, M.A., and Willis, D.G., 1967. The Elastic Coefficients of the Theory of Consolidation, Jour. of Applied Mechanics, pp. 594.

Bredehoeft, J.D., Wolff, R.G., Keys, W.S., and Shuter, E., 1976. Hydraulic Fracturing to Determine the Regional In Situ Stress Field, Piceance Basin, Colorado, Geol. Soc. of America Bull., Vol. 87, p. 250 - 258.

Clark, J.B., 1949. A Hydraulic Process for Increasing the Productivity of Wells, Petroleum Transactions, AIME, Vol. 186, pp. 1 - 8.

Daneshy, A.A., 1973a. A Study of Inclined Hydraulic Fractures, Soc. of Petroleum Engineers Jour., April, pp. 61 - 68.

Daneshy, A.A., 1973b. Experimental Investigation of Hydraulic Fracturing Through Perforations, Jour. of Petroleum Technology, October, pp. 1201 - 1206.

Daneshy, A.A., 1974. Hydraulic Fracture Propagation in the Presence of Planes of Weakness, Soc. of Petroleum Engineers Paper SPE 4852, 8 p.

Daneshy, A.A., 1978. Hydraulic Fracture Propagation in Layered Formations, Soc. of Petroleum Engineers Jour., February, pp. 33 - 51.

Dunn, D.E., Donaldson, M., and Huf, W.E., 1978. Evaluation of Transient Pore Pressures in Hydraulic Fracturing of Sandstone and Shale, in Proceedings of 19th Symposium on Rock Mechanics, Vol. 1, May 1-3, pp. 319-326.

Fairhurst, C., 1964. Measurement of In Situ Rock Stresses, with Particular Reference to Hydraulic Fracturing, Rock Mechanics and Engrg. Geology, Vol. 1-2, pp. 129-147.

Haimson, B., 1968. Hydraulic Fracturing in Porous and Nonporous Rock and its Potential for Determining In Situ Stresses at Great Depth, Ph.D. Thesis, University of Minnesota, Minneapolis, Minnesota, 234 p.

Haimson, B., and Fairhurst, C., 1969. Hydraulic Fracturing in Porous - Permeable Materials, Jour. of Petroleum Technology, July, pp. 811-817.

Haimson, B., 1974. Determination of In-Situ Stresses Around Underground Excavations by Means of Hydraulic Fracturing, Technical Report, Dept. of Metallurgical and Mineral Engineering and the Engineering Experiment Station, University of Wisconsin, Madison, Wis., 101 p.

Haimson, B., 1975. Deep In Situ Stress Measurements by Hydrofracturing, Tectonophysics, Vol. 29, pp. 41-47.

Haimson, B., 1976. The Hydrofracturing Stress Measuring Technique - Method and Recent Field Results in the U.S., in Proceedings of 18th U.S. Symposium on Rock Mechanics, pp. 4C2 1 - 4C2 6.

Haimson, B., 1978a. Crustal Stresses in the Michigan Basin, Jour. of Geophys. Res., Vol. 83, pp. 5857-5863.

Haimson, D., 1978b. Near-Surface and Deep Hydrofracturing Stress Measurements in the Waterloo Quartzite, in Proceedings of 19th Symposium on Rock Mechanics, pp. 345-361.

Hubbert, M.K., and Willis, D.G., 1957. Mechanics of Hydraulic Fracturing, Transactions of AIME, Vol. 210, pp. 153-160.

Jaeger, J.C., and Cook, N.G.W., 1976, Fundamentals of Rock Mechanics, John Wiley, New York, 585 p.

Kehle, R.O., 1964. The Determination of Tectonic Stresses Through Analysis of Hydraulic Well Fracturing, Jour. of Geophys. Res., Vol. 69, pp. 259-273.

Medlin, W.L., and Masse, L., 1976. Laboratory Investigation of Fracture Initiation Pressure and Orientation, Soc. of Petroleum Engineers Paper SPE 6087, 24 p.

Scheidegger, A.E., 1962. Stresses in the Earth's Crust as Determined from Hydraulic Fracturing Data, Geologie und Bawvasen, Vol. 27, pp. 45-60.

Sun, R.J., 1969. Theoretical Size of Hydraulically Induced Horizontal Fractures and Corresponding Surface Uplift in an Idealized Medium, Jour. of Geophys. Res., Vol. 74, pp. 5995-6011.

Sun, R.J., 1972. Discussion of "Natural and Induced Fracture Orientation" by M.K. Hubbert, in Underground Waste Management and Environmental Implications, American Assoc. of Petroleum Geologist Memoir 18, pp. 237.

Sun, R.J., 1978. Hydraulic Fracturing as a Tool for Disposal of Wastes in Shale (abst.), American Assoc. of Petroleum Geologist Bull., Vol. 57, pp. 1606.

Terzaghi, K., 1943. Theoretical Soil Mechanics, John Wiley, New York, 510 p.

Zoback, M.D. and Pollard, D.D., 1978. Hydraulic Fracture Propagation and the Interpretation of Pressure-Time Records for In Situ Stress Determinations, in Proceedings of 19th Symposium on Rock Mechanics, Vol. 1, May 1-3, pp. 14-22.

APPENDIX I

COMPUTER PROGRAM FOR HYDRAULIC FRACTURING TESTS

This Basic program was written to run hydraulic fracturing tests (with either the nipple or straddle packer) on an MTS test system interfaced with a Digital pdp 11/04 computer. The system contains two channels which are used here to operate the load frame and a pressure intensifier (see Fig. 9). Both the load frame and pressure intensifier generate compressive pressures with negative valued commands. Feedback is provided for channel one (pressure intensifier) by a pressure transducer. Channel two (load frame) is governed by feedback from a load cell.

On channel one, the borehole pressure transducer is kept in control throughout the test. Confining pressure and acoustic emissions can, though, be monitored by channel one.

Subroutines for plotting, data storage, or data printout are separate Basic programs. These subroutines are made part of the main program through the OVERLAY statement. This facilitates multiple use of the plotting and data handling routines and conservation of core space in the working memory.

```
HYDFAC   MTS BASIC V01B-02

70 REM PROGRAM TO SIMULATE IN-FIELD HYDRAULIC FRACTURING
75 REM AXIAL LOAD - HSG1,CH 2; BOREHOLE PRESS,
76 REM CONFINING PRESS AND ACOUSTIC EMISSIONS -
77 REM HSG1,CH 1.
90 QUIT\CNTR(3)
170 PRINT "DOES SYSTEM HAVE XCDR 1 (CHANNEL 0) IN CONTROL ?"
172 PRINT "IF NOT MANUALLY SWITCH NOW, PRESS RETURN";\INPUT S$
180 PRINT "APPLY SMALL AXIAL LOAD MANUALLY, RETURN";\INPUT H$
190 PRINT "APPLY SMALL CONF PRESS MANUALLY, RETURN";\INPUT J$
200 PRINT "ZERO TRANSDUCERS AS CLOSELY AS POSSIBLE, RETURN";\INPUT A$
210 DIM X(207),Y(207),Z(71)
220 DIM T1(25),S4(25),C4(25),P4(25),E4(25)
225 DIM T(300),S(300),C(300),P(300),E(300)
230 DIM L(8)
240 PRINT "ENTER ROCK ID";\INPUT R0$
250 C0$=R0$&"^"&DAT$
260 PRINT "ENTER ROCK DIAMETER";\INPUT D9
265 PRINT "ENTER BOREHOLE DIAMETER";\INPUT D7
270 PRINT "ENTER FULL SCALE AXIAL LOAD";\INPUT A9
280 PRINT "ENTER FULL SCALE CONF PRESS";\INPUT C9
290 PRINT "ENTER FULL SCALE BOREHOLE PRESS";\INPUT P9
295 PRINT "ENTER FULL SCALE ACOUSTIC EMISSION RDC";\INPUT E9
300 PRINT "ENTER FILE NAME DESIGNATION";\INPUT Z$
310 Z$="DX1:"&Z$
320 PRINT "ENTER DESIRED OPERATING AXIAL STRESS";\INPUT R9
330 PRINT "ENTER DESIRED OPERATING CONF PRESS";\INPUT R2
335 REM SET LOADING FACTORS
342 R0=R9*(((PI*D9^2)/4)-((PI*D7^2)/4))
350 M2=-(R0/A9)*2047
360 N2=-(R2/P9)*2047
370 REM BUILD RAMP TO APPLY AXIAL LOAD AND CONF PRESS
380 X=205
390 X(1)=409
400 FOR I=2 TO 204 STEP 2
410 X(I)=-10*(I-1)
420 X(I+1)=X(I)
430 IF X(I)>N2 GO TO 450
440 X(I)=N2
450 IF X(I+1)>M2 GO TO 470
460 X(I+1)=M2
470 NEXT I
500 REM BUILD RAMP TO APPLY BOREHOLE PRESS
510 Y=205
```

```
520 Y(1)=256
530 FOR I=2 TO 204 STEP 2
540 Y(I)=-10*(I-1)
550 Y(I+1)=M2
555 NEXT I
560 REM BUILD RAMP TO BACK OFF PORESS INTENSIFIER
561 Z=71
562 Z(1)=256
563 FOR I=2 TO 70 STEP 2
564 Z(I)=N2+(15*(I-1))
565 Z(I+1)=M2
566 IF Z(I+1)>0 THEN 568
567 GO TO 572
568 Z(I)=Z(I-2)-5
569 IF Z(I)>-15 THEN 572
570 Z(I)=-15
572 NEXT I
575 REM SET PLOTTING SCALE FACTORS
580 C1=C9/2047\P1=P9/2047\E1=E9/2047
590 S1=A9*4/(((PI*D9^2)-(PI*D7^2))*2047)
600 TIME (1000)
720 DACQ(3,P4,0,10)
730 DACQ(6,C4,1,0)
740 DACQ(6,S4,4,0)
750 DACQ(6,E4,2,0)
760 DACQ(7,T1,0,0)
765 CNTR(3)
770 PRINT "CLOSE BOREHOLE VALVE; OPEN CONF VALVE"
771 FOR I+1 TO 10000\NEXT I
772 PRINT " "
773 PRINT "ARE VALVES ADJUSTED (YES OR NO)";\INPUT C$
774 IF C$<>"YES" GO TO 771
780 CNTR(3)\PRINT "PRESS RETURN TO BEGIN";\INPUT C$
790 STAR
800 FG1(X,1,7,2) -
810 FOR I=1 TO 3000\NEXT I\CNTR(3)
811 PRINT "TIME","CONFPRESS","BOREHOLE","LOAD"
812 FOR I=1 TO 25
813 PRINT T1(I),C4(I),P4(I),S4(I)
814 NEXT I
820 PRINT "ARE LOAD AND CONF PRESS CONSTANT";\INPUT D$
830 IF D$="NO" THEN 810
840 IF D$<>"YES" THEN 820
841 R=C4
846 PRINT "DATA POINTS TAKEN = ";R
848 PRINT " "
```

```
850 PRINT "CLOSE CONF PRESS VALVE"
851 FOR I=1 TO 15000\NEXT I
852 PRINT " "
853 PRINT "ARE VALVES ADJUSTED (YES OR NO)";\INPUT C$
854 IF C$<>"YES" THEN 851
859 CNTR(3)
860 PRINT "TO RETURN PRESS INT TO ZERO PRESS RETURN";\INPUT D$
865 FG1(Z,1,7,2)
870 FOR I=1 TO 5000\NEXT I\CNTR(3)
872 PRINT "SET STRADDLE PACKER"
873 FOR I=1 TO 5000\NEXT I\PRINT " "
874 PRINT "IS PACKER SET (YES OR NO)";\INPUT D$
875 IF D$<>"YES" THEN 873
876 CNTR(3)
880 PRINT "OPEN BOREHOLE VALVE"
881 FOR I=1 TO 5000\NEXT I
882 PRINT " "
883 PRINT "ARE VALVES ADJUSTED (YES OR NO)";\INPUT C$
884 IF C$<>"YES" THEN 881
889 CNTR(3)
890 PRINT "PRESSURIZE BOREHOLE WITH RETURN KEY";\INPUT F$
895 QUIT
910 DACQ(3,P,0,4)
920 DACQ(6,S,4,0)
930 DACQ(6,C,1,0)
933 DACQ(6,E,2,0)
935 DACQ(7,T,0,0)
936 STAR
940 FG1(Y,1,7,4)
945 G5=0
950 IF G5>0 THEN 980
951 CNTR(3)\PRINT "STOP FUNCTION GENERATION (YES OR NO)";\INPUT H$
952 IF H$<>"YES THEN 954
953 FG1(-1)
954 PRINT "STOP TAKING DATA (YES OR NO)";\INPUT G$
955 IF G$ ="NO" THEN 975
958 IF G$<>"YES" THEN 950
960 P2=P+R\QUIT\G5=G5+1\GO TO 976
975 P2=P+R
976 IF P2<325 THEN 980
977 P2=325
979 REM CHOOSE PLOT
980 PRINT "DATA POINTS TAKEN = ";P2
990 PRINT "AXIAL LOAD VS TIME - 1"
1000 PRINT "CONFINING PRESS VS TIME - 2"
1010 PRINT "BOREHOLE PRESS VS TIME - 3"
```

```
1020 PRINT "ACOUSTIC EMISSION VS TIME - 4"
1030 PRINT "TO DETERMINE BOREHOLE BREAKDOWN PRESS - 5"
1060 PRINT "TO STORE DATA - 7"
1070 PRINT "TO PRINT OUT DATA - 8"
1080 PRINT "TO STOP PROGRAM - 9"
1085 INPUT L
1090 ON L GO TO 2000,2002,2004,2006,2008,2014,2010,2012,3430
1095 GO TO 950
2000 OVERLAY "DX1:PLOT 1"
2001 GO TO 2050
2002 OVERLAY "DX1:PLOT 2"
2003 GO TO 2050
2004 OVERLAY "DX1:PLOT 3"
2005 GO TO 2050
2006 OVERLAY "DX1:PLOT 4"
2007 GO TO 2050
2008 OVERLAY "DX1:PLOT 3"
2009 GO TO 2050
2010 OVERLAY "DX1:STORE"
2011 GO TO 2050
2012 OVERLAY "DX1:PRINT"
2013 GO TO 2050
2014 OVERLAY "DX1:PLOT 5"
2015 GO TO 2050
3090 REM SUBROUTINE TO DETERMINE BOREHOLE BREAKDOWN PRESS
3100 CPOS(T3,P3)\COMM("----------PF",T3,P3)
3110 CPOS(T4,P4)\CNTR(3)
3130 PRINT "BOREHOLE BREAKDOWN PRESSURE = ";P3;"PSI"\PRINT " "
3140 GO TO 950
3190 REM SUBROUTINE TO PLACE PLOT TITLE
3200 CPOS(X9,Y9)\COMM(C0$,X9,Y9)
3210 CPOS(X9,Y9)\CNTR(3)
3220 GO TO 950
3430 QUIT\STOP
```

```
PLOT1        MTS BASIC V01B-02


2050 REM PLOT AXIAL LOAD VS TIME
2060 K=P2\CNTR(3)
2070 T2=1
2080 FOR I=1 TO R
2090 T2=T2+T1(I)
2100 NEXT I
2110 FOR J=1 TO K-R
2120 T2=T2+T(J)
2130 NEXT J
2140 PHYL(100,950,55,750)
2150 SCAL(0,0,.1*T2,0,(4*R0/(D9^2*PI))+300)
2160 AXES(0,0)
2170 A$="AXIAL LOAD (PSI)"
2180 T$="TIME (SEC)"
2190 LABL(T$,A$,15,150,1)
2200 T3=0
2210 FOR I=1 TO K
2220 IF I>R THEN 2260
2230 T3=T3+T1(I)
2240 PLOT(.1*T3,-S1*S4(I))
2250 GO TO 2290
2260 L=I-R
2270 T3=T3+T(L)
2280 PLOT(.1*T3,-S1*S(L))
2290 NEXT I
2300 GO TO 3200
```

```
PLOT2      MTS BASIC V01B-02


2050 REM PLOT CONFINING PRESSURE VS TIME
2060 K=P2\CNTR(3)
2070 T2=1
2080 FOR I=1 TO R
2090 T2=T2+T1(I)
2100 NEXT I
2110 FOR J=1 TO K-R
2120 T2=T2+T(J)
2130 NEXT J
2140 PHYL(100,950,55,750)
2150 SCAL(0,0,.1*T2,0,R2+100)
2160 AXES(0,0)
2170 C$="CONFINING PRESSURE (PSI)"
2180 T$="TIME (SEC)"
2190 LABL(T$,C$,15,25,1)
2200 T3=0
2210 FOR I=1 TO K
2220 IF I>R THEN 2260
2230 T3=T3+T1(I)
2240 PLOT(.1*T3,-C1*C4(I))
2250 GO TO 2290
2260 L=I-R
2270 T3=T3+T(L)
2280 PLOT(.1*T3,-C1*C(L))
2290 NEXT I
2300 GO TO 2300
```

```
PLOT3      MTS BASIC V01B-02

2050 REM PLOT BOREHOLE PRESSURE VS TIME
2060 K=P2\L2=L\CNTR(3)
2070 T2=1
2080 FOR I=1 TO R
2090 T2=T2+T1(I)
2100 NEXT I
2110 FOR J=1 TO K-R
2120 T2=T2+T(J)
2130 NEXT J
2140 PHYL(100,950,55,750)
2150 SCAL(0,0,.1*T2,0,P9)
2160 AXES(0,0)
2170 P$="BOREHOLE PRESSURE (PSI)"
2180 T$="TIME (SEC)"
2190 LABL(T$,P$,15,300,1)
2200 T3=0
2210 FOR I=1 TO K
2220 IF I>R THEN 2270
2230 T3=T3+T1(I)
2240 P4(I)=0
2250 PLOT(.1*T3,-P1*P4(I))
2260 GO TO 2300
2270 L=I-R
2280 T3=T3+T(L)
2290 PLOT(.1*T3,-P1*P(L))
2300 NEXT I
2310 IF L2=5 THEN 3100
2320 GO TO 3200
2300 GO TO 2300
```

```
STORE    MTS BASIC V01B-02


2050 REM TO STORE DATA
2060 QUIT\FG1(-1)
2070 K=P2\CNTR(3)
2080 OPEN Z$ FOR OUTPUT AS FILE VF1
2090 VF1(0)=K
2100 FOR I=1 TO R
2110 VF1(I)=S4(I)
2120 VF1(K+I)=C4(I)
2130 VF1(2*K+I)=P4(I)
2140 VF1(3*K+I)=E4(I)
2150 VF1(4*K+I)=T1(I)
2160 NEXT I
2170 FOR I=R+1 TO K
2180 VF1(I)=S(I=R)
2190 VF1(K+I)=C(I-R)
2200 VF1(2*K+I)=P(I-R)
2210 VF1(3*K+I)=E(I-R)
2220 VF1(4*K+I)=T(I-R)
2230 NEXT I
2240 CLOSE
2250 GO TO 950
2290 PLOT(.1*T3,-P1*P(L))
2300 NEXT I
2310 IF L2=5 THEN 3100
2320 GO TO 3200
2300 GO TO 2300
```

```
PRINT    MTS BASIC V01B-02


2050 REM PRINT STORED DATA
2060 OPEN Z$ FOR INPUT AS FILE VF1
2070 K=VF1(0)
2080 PRINT "LOAD","CONF PRES","BORHL PRES","ACOUSTIC","TIME"
2090 FOR I=1 TO K
2100 PRINT VF1(I),VF1(K+I),VF1(2*K+I),VF1(3*K+I),VF1(4*K+I)
2110 NEXT I
2120 CLOSE
2130 GO TO 950
```

APPENDIX II

HYDRAULIC FRACTURING TENSILE STRENGTH IN DOW/ERDA WELL 100 CORES

Hydraulic fracturing tests were performed on samples obtained from Dow Chemical's Dow/ERDA well 100 located in Sanilac County, Michigan. Several drawbacks were encountered in using the cores, however. Each sample obtained from the core was from a different mineralogic horizon, thus making sample to sample data comparison difficult. Secondly, the number of samples from these cores was limited as previous research on the Antrim Shale had diminished the number of long core sections (> 5 inches in length) by the time this study was initiated.

Dow/ERDA well 100 cores (3-1/2 inches in diameter) were fractured using the miniature straddle packer. Since each core represented a different mineralogic horizon, plots similar to those for the quarry block samples would be meaningless. Unconfined testing of all the cores, however, resulted in a measure of the hydraulic fracturing tensile strength in the plane of bedding (T_2). This was plotted against depth to show the variation of tensile strength throughout the thickness of the Antrim formation.

Orientation marks on the Dow cores were small grooves running the full length of each sample. These marks were carved into the cylindrical walls of the core during drilling. Stress concentration of the external load due to these grooves was only present in the outer 1/4 inch of the diameter of each sample (by Saint-Venant's principle). Thus, failure pressures from breakdown at the borehole wall, were uneffected by these grooves. The fracture directions, however, were strongly influenced by the orientation grooves.

Axial load and initial packer set-pressure were 1500 and 300 psi, respectively. With the exception of two cores, all failures were vertically oriented. One of these was an inclined fracture plane which was oriented approximately 45° to the borehole axis. The other exception was a horizontal failure which occurred in a prefractured sample.

Vertical breakdown pressures were recorded (Table AII-1) and plotted against well depth in Figure AII-1 to show the variation in tensile strength T_2 throughout the thickness of the formation.

Figure AII-2a shows typical fracture planes including several examples of failure planes that were altered during their growth. These planes met the cylindrical sample wall along the orientation groove. The Dow/ERDA cores also showed the only examples of branching fractures observed during this study (Fig. AII-2b).

Results from Dow/ERDA well 100 samples (Fig. AII-1) show an increasing tensile strength in the plane of bedding throughout the top two-thirds of the Antrim formation. Near 1375 feet, the tensile strength T_2 reaches a maximum value of approximately 3900 psi. The next data points, from the 1400 to 1450 foot level, indicate an average tensile strength of about 2000 psi. This distinct change in the nature of the Antrim corresponds with Bennett's (1978) contact between lithofacies III and lithofacies IV.

Lithofacies IV (1210 to 1370 feet) was deposited in the deepest waters which prevailed in Upper Devonian times (Bennett, 1978). The continual sediment build-up and the large hydrostatic load caused this lithofacies to be more compacted at its base. This differential compaction explains the increasing tensile strength trend seen throughout the thickness of lithofacies IV.

TABLE AII-1

Hydraulic Fracturing Results for Unconfined Tests on 3-1/2 inch Antrim Shale Cores from Dow/ERDA Well 100 (1500 psi Axial Stress, All Vertical Fractures except as noted).

Sample Depth (ft)	Breakdown Pressure (psi)	Sample Depth (ft)	Breakdown Pressure (psi)
1232.4	1090	1365.8	3480
1242.1	950	1409.0	1860
1248.0	1680	1415.1	2036
1308.5	1840	1416.2	1900
1308.7	1170	1417.2	1960
1313.2	2900	1421.2	1490
1349.3*	1170	1426.1	2410
1358.0	4700	1428.5	2360
1365.0†	3310	1429.8	2080

*Inclined fracture plane (approximately 45° to the borehole axis)

†Horizontal fracture plane (prefractured sample)

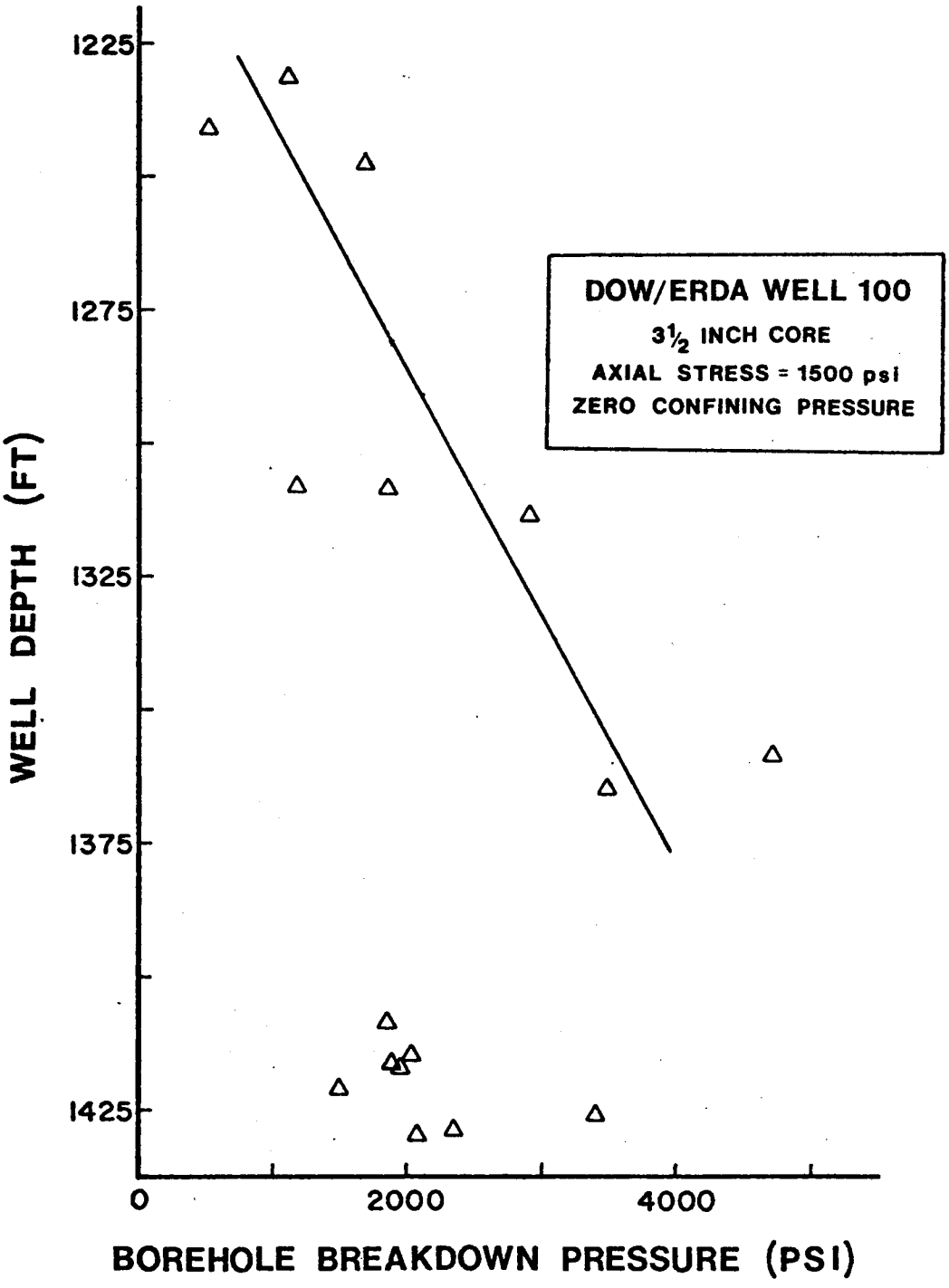

Figure AII-1. Vertical hydraulic fracturing tensile strength measurement with depth for Antrim Shale.

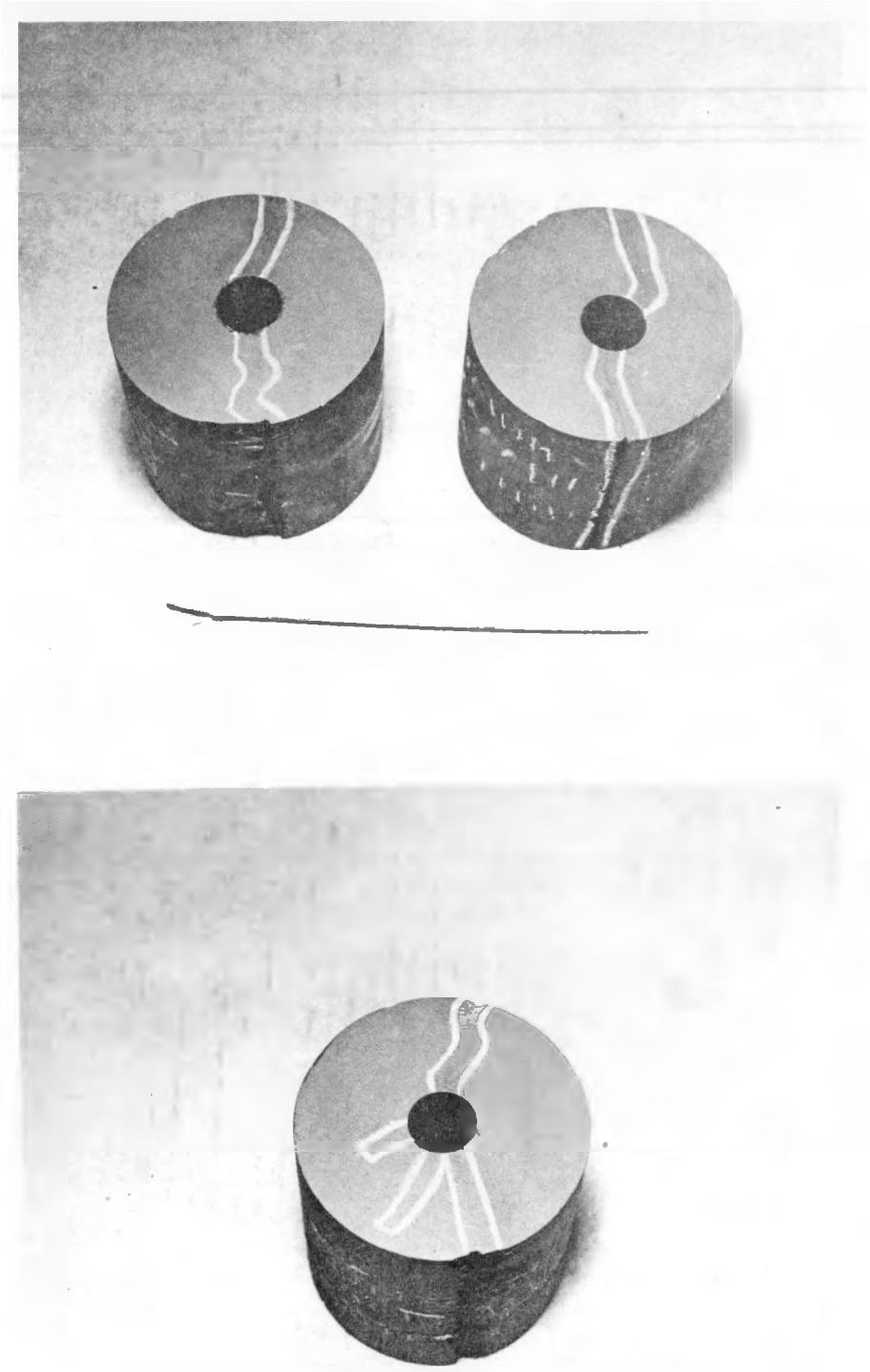

Figure AII-2 a) Vertical fracture planes in Dow/ERDA well 100 cores. Orientation grooves altering failure plane direction. b) Branching fracture plane.

☆U.S. GOVERNMENT PRINTING OFFICE: 1980–640-258/2188